Using Remote Sensing to Determine Differences in Soybean Seeding Rates

A Thesis

Submitted to the Faculty

of

Purdue University
by

Jared Alsdorf

In Partial Fulfillment of the

Requirements for the Degree

of

Master of Science

May 2007

Dedication

Acknowledgements

Table of Contents

List of Tables

List of Figures

Abstract

The use of vegetative indices has been useful for measuring differences in crop canopy characteristics such as leaf are index, plant density, photosynthetically active biomass, chlorophyll content, wet and dry biomass, plant height and yield. This research focuses on the ability of vegetation indices to determine differences in soybean seeding rates. It is assumed that biomass increases with seeding rates and can be measured using remote sensing Field studies were conducted over a three year period in Central Indiana. Three row spacing treatments were tested using nine seeding rates ranging from 0 to 1,000,000 seeds per hectare. Numerous indices were tested using a linear, quadratic and polynomial regression. The normalized red indice (Norm R) with a polynomial regression model correlated nicely with soybean seeding rates. This combination was consistent between and across treatments. Analyses of R^2 values by crop growth stage and treatments show the crop growth stage between V7 and R2 show the best correlation for soybean seeding rates. The results of this study are consistent with research showing that remote sensing and vegetation indices are useful for determining differences in plant biomass.

Introduction

Vegetation indices have been developed to reduce multi-band observations into a single dimensionless radiometric number in order to enhance green vegetation while normalizing the effects of soil and variations in atmospheric conditions (Jensen, 2005; Weigand and Richardson, 1990; Weigand et al., 1991).

Vegetation indices were first reported by Jordan (1969) who used a ratio vegetation index (RVI) to measure differences in forest canopies. In 1973 Rouse et al., conducted a study to develop a quantitative measurement for above ground biomass in rangelands. Bands 5 and 7 form the ERTS-1 were recorded and used to develop what is know today as the normalized difference vegetation index (NDVI). Research by Tucker (1979) used linear combinations of red-infrared bands and green-infrared bands to quantify differences in plant biomass, leaf water content and chlorophyll content. From this study additional red-infrared band combinations, most notably the difference vegetation index (DVI) and ratio vegetation index (RVI) were developed. In 1996 Giletson et al. studied the feasibility of indices using the simulated green channel (550nm) of the EOS-MODIS satellite. A new indice, called the green normalized difference vegetation index (GNDVI) was developed based on the NDVI in which the red band was replaced by the green band.

The red-infrared indices correlate well with foliage density as a function of biomass, but remain sensitive to soil background and atmospheric affects (Rondeaux et al., 1991). In an attempt to minimize these effects Huete (1988) developed the soil adjusted vegetation index (SAVI) by modifying the NDVI indice. A soil-adjustment factor L was added to account for the first-order soil background. An adjustment factor of

L=0.5 is the standard since it is normally larger that the red reflectance value and would still buffer for soil reflectance. The SAVI was modified by Qi et al. (1994) resulting in a new index called the modified soil adjusted vegetation index (MSAVI). The MSAVI is said to be an improvement over the SAVI in that is replaces the constant variable L with a variable L function that accounts for variation between soils and the range of vegetation cover from very sparse to a very dense canopy.

In an attempt reduce atmospheric affects Kaufman and Tanré (1992) added the blue channel in combination with the red channel such as NDVI in order to create atmospherically resistant vegetation index (ARVI). This same process can also be applied to the SAVI and the TSAVI by changing the G to GB in the index (Rondeaux, 1996). The disadvantage of this process is that these indices minimize the soil and atmospheric effects independently but fail to correct for these variables when applied simultaneously (Myeni and Asrar, 1994).

Numerous studies have been conducted in the past three decades to develop applications for these vegetation indices as well as develop new indices. Most of the work done with vegetation indices focuses on the characteristics of crop canopies such as leaf area index, plant density, photosynthetically active biomass, chlorophyll content, wet and dry biomass, plant height and yield (Baret and Guyot, 1990; Clevers, 1989; Jones and Holshouser, 2001; Purevdorj, 1998; Senay et al., 2000; Thenkabail et al., 1992; Thenkabail et al., 1994a, Thenkabail et al., 1994b; Tucker, (1979); Wiegand et al., 1990; Wiegand et al. 1991a; Wiegand et al. 1991b).

A review of these studies shows that vegetation indices are useful for determining differences in crop canopies as a function of biomass. However, little research has been conducted to evaluate the ability of these techniques to measure differences in seeding rates for agricultural crops as a function of plant biomass. The goal of this research is to see how accurately soybean seeding rates can be determined using color infrared imagery.

The specific objectives of this study were to:

1. Identify vegetation indices that can be used to detect differences in soybean seeding rates.
2. Build an algorithm that can be used to measure these differences.
3. Develop an image library specific to soybean seeding rates.

Literature Review

Applications of Remote Sensing in Agriculture

Remote sensing technology has been used successfully in agriculture starting with the inception of the Landsat satellite program in the early 1970's (Shao, 2004). The Lansdat program provided a platform for the Large Area Crop Inventory Experiment (LACIE) starting in the late 1970s which was used to estimate wheat production (Moran et. al., 1997). These efforts were soon followed by the AgRISTARS program which along with the LACIE program extended the methodology to other crops and defined the biological and physical properties of crop canopies and soils. Since this time numerous other satellite programs such as SPOT, IKONOS and Quickbird have proved useful for agriculture. The continued success of this technology is dependent on the development and deployment of low cost sensors that provide better resolution, revisit times, delivery schedules and cost. Numerous sensors that are designed to address these issues are scheduled to be launched in the next two years (Table 1).

Table 1. Planned launche of remote sensing satellites for 2007-2008 (Stoney, 2006)

Satellite	**Country**	**Launch**	**Best Resolution (m)**
GeoEye-1	USA	03/2007	1.64
WorldView-1	USA	07/2007	0.5
WorldView-2	USA	07/2008	0.5
EROS C	Isreal	03/2008	2.5
Pleiades-1	France	07/2008	2.5
Thoes	Thialand	06/2007	8
RapidEye 1-6	Germany	07/2007	6.5

The RapidEye program is of interest because five sensors will be launched at once. Each sensor will provide a spatial resolution of 6.5 meters with a spectral resolution of five bands and a temporal resolution of one day. Included in this spectral resolution will be the first red edge band (Figure 1).

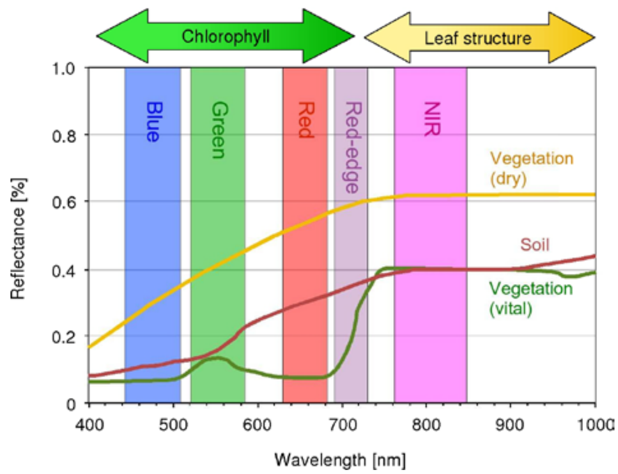

Figure 1. Spectral resolution of Rapid Eye sensors (Hansen, 2006)

Remote sensing has numerous applications for agriculture. These range from field mapping for the establishment of the USDA/FSA common and unit (CLU) to monitoring the effects of biotechnology. Nitrogen management and yield predictions are two applications of remote sensing that interest me. This section will focus on these two applications.

The ability to predict yield prior to harvest is valuable to growers as they develop marketing plans for their grain. It is also an important tool for the crop insurance industry as they settle claims. The process for determining yield estimations in crops is the integration of models related to Leaf Area Index (LAI) or percent vegetative (Moran et all., 1997). Research done by Chang et al, (2003) reports that canopy reflectance measurements using aerial and IKONOS images account for 45% of the yield variability in corn. He also reports in this research that studies by Hong, using principal-component analysis, was able to explain 70% of corn yield variability.

Ma et al, (2001) conducted research to determine soybean yield using a hand-held radiometer. Data for this study suggests that using NDVI to measure canopy reflectance, between the R4 and R5 growth stage is a good indicator of yield. R^2 values ranged from 0.44-0.80.

Numerous companies in the industry are having success marketing and selling yield prediction products in spite of these differences reported in the research (Bechman, 2002) (Knoblauch, 2007).

Another application of remote sensing is nitrogen management. As nitrogen prices continue to increase many growers are looking for ways to improve nitrogen efficiency and management practices. A number of new on-the-go sensors such as the GreenSeeker® (NTech Industries, Ukiah, CA) use NDVI indices to create nitrogen recommendation maps. Areas in the field with low NDVI values receive more nitrogen than areas with high NDVI values.

Numerous research projects have been done using airborne sensors to monitor nitrogen stress. Scharf (2002) used color and infrared film sensors to collect photographs of corn at the V6-V7 growth stages. The results from this study showed that color images were more accurate (R^2 = 0.27-0.31) than infrared for predicting nitrogen stress. The success of the color imagery was greatly increased when the soil back ground was removed (R^2 = 0.60-0.79) and high-N reference strips were included. In 2005 Sripada et al. used three channel (green, red and near-infrared) photographs to determine if there was a corn response to nitrogen applications pre-tassel (VT) and to develop a methodology for predicting N requirements at this growth stage. The results from this study showed that green difference vegetation index (GNDVI) was the best predictor of nitrogen requirements (R^2=0.67) when used with high-N reference strips.

Additional research by Ahmad et al., (1999); Clay et al., (2006); Lee et. al. (1999); Lee at al., (2000); Teal et al., (2004); Wright et al., (2004) in addition to others has shown that leaf chlorophyll content is a good predictor of leaf nitrogen content and that vegetative indices such as NDVI are useful for determining nitrogen needs.

The Science of Remote Sensing

The sun emits energy in the form of photons which is measured and quantified into wavelengths using the electromagnetic spectrum. The electromagnetic spectrum covers a wide range of wavelengths starting with the very short gamma rays to the long radio waves. The visible light range is a narrow portion of the spectrum between 400-700nm (Figure 2). The visible spectrum along with the infrared spectrum (700-3000 nm) provide the impetus for remote sensing.

Solar radiation from the sun passes through the atmosphere to the earth's surface. Along the way atmospheric components interact with this radiation by absorbing, scattering or refracting a portion of this energy. The remaining energy is transmitted to the earth's surface where it is absorbed, transmitted or reflected (Figure 3).

The ability of radiation to pass through the atmosphere is a function of wavelength. Certain wavelengths are able to pass relatively unimpeded in the atmosphere through what are called 'atmospheric windows" while others are partially or totally blocked (Figure 4).

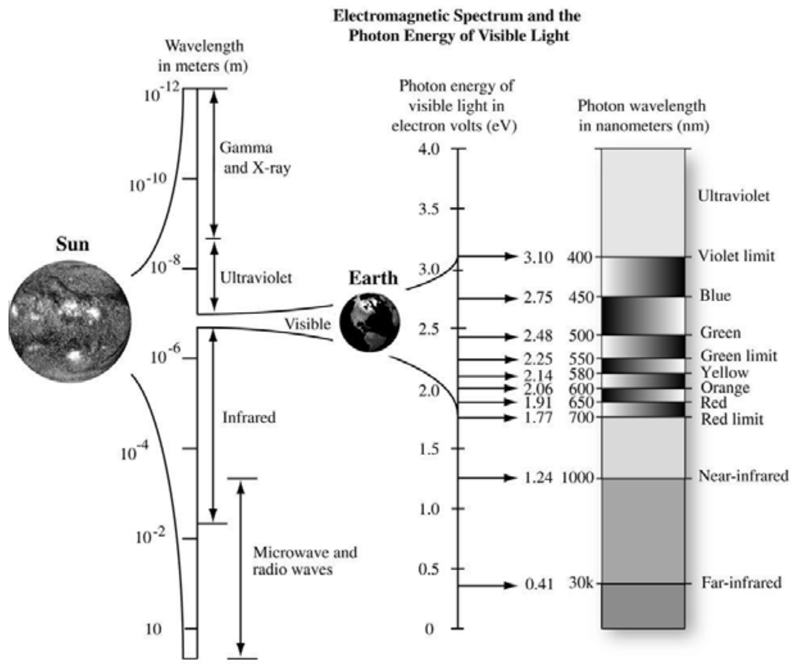

Figure 2. Electromagnetic Spectrum (Jensen 2005)

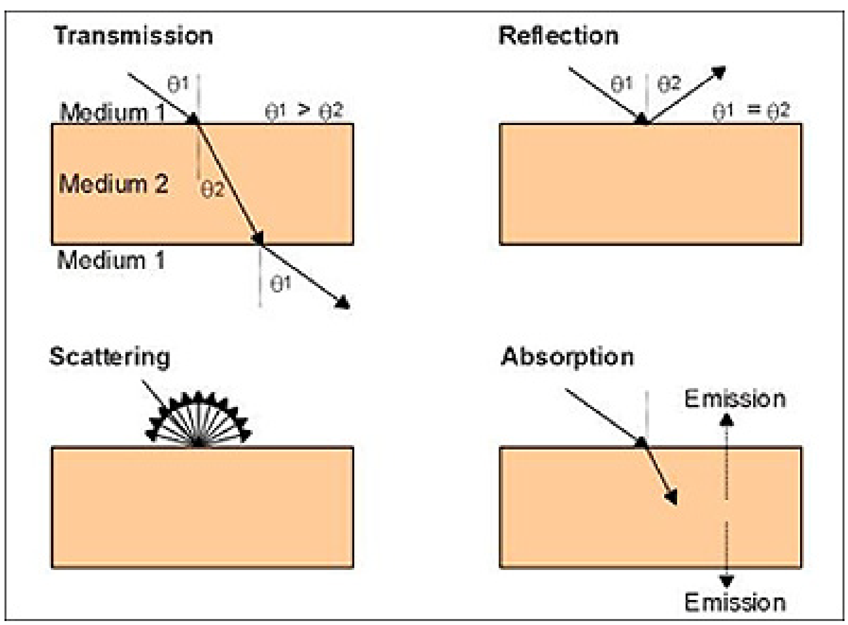

Figure 3. The spectral response of energy on a target (Short, 2007).

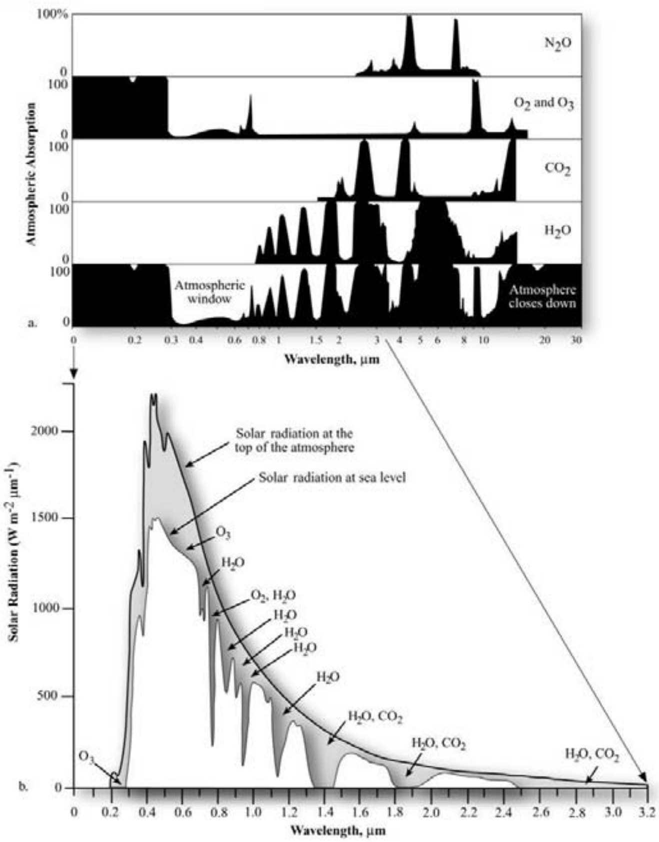

Figure 4. Atmospheric transmittance in the visible and infrared spectrum (Jensen, 2005)

Remote sensing devices work by measuring the amount of radiation that is reflected from the surface of an object. Passive sensors, such as the AVIRIS, measure reflected solar energy and are designed to work within the ‘atmospheric windows’. Additive radiation from atmospheric scattering adds information to passive sensors creating “noise” in the image. Environmental factors, such as haze, can diminish the spectral return resulting in a dark image. Active sensors, such as radars, beam out generated energy and measure the portion that is reflected back. The advantage of this system is the ability to work in the absence of light or under cloud cover (Shao, 2004).

Remote Sensing of Agronomic Crops

Light Interaction with Leaves

Radiant energy from the sun is used by leaves to power photosynthesis and other physiological processes. As radiant energy strikes the surface of the leaf, a portion is reflected while the rest is absorbed or transmitted. These energy responses are interrelated and must be considered together when evaluating spectral response of vegetation (Knipling, 1970) as seen in Figure 5.

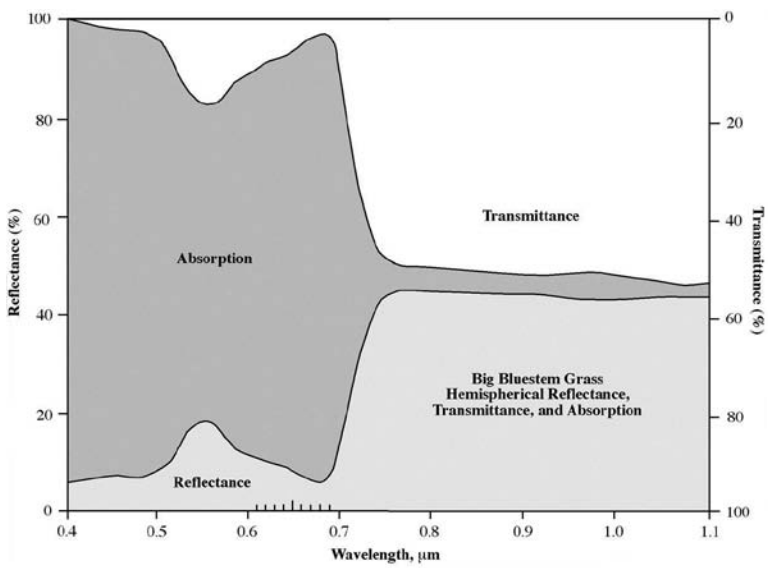

Figure 5. Relationship of absorption, reflectance and transmittance (Jensen 2005)

The energy response in leaves is a function of cellular structure and cellular components. The cellular structure of most leaves is composed of the epidermis, palaside parenchyma cells in the upper mesophyll, irregular loosely arranged spongy parenchyma cells in the lower mesophyll, chloroplasts in the palaside parenchyma cells and intercellular space (Jensen, 2005). In planophile cells the palisade cells are located on the upper surface of the leaves and in erectophile they are located on both sides (Volenec, 2007). The cellular components are cellulose in the cell walls, water containing solutes within cells, inter-cellular air spaces and pigments in the chloroplasts (Gates et. al., 1965). As solar energy interacts with these components the response is measured in three regions of the electromagnetic spectrum:

1. The visible wavelengths from 400-700 nm are generally referred to as photosynthetically active radiation (PAR) which is the solar radiation used for photosynthesis. Reflectance in this portion of the spectrum is very low, around 10%, with a peak at 550nm in the green region. Low reflectance is due to high absorption by plant pigments, primarily chlorophyll and carotenoids. As leaves age or become stressed, reflectance increases due to decreasing levels of chlorophyll.
2. The near infrared wavelengths from 700-1,300nm are not absorbed by vegetation and reflect around 50%, while the other 50% is transmitted downward through the leaf and reflected again by the lower leaves in a process called leaf additive reflectance (Sinclair et al., 1971). Reflection and transmittance of infrared energy are mirror images of each other (Figure 5) and are affected by the inter-cellular space in the spongy mesophyll layer. Any change to the internal leaf structure will influence the infrared reflectance. Knipling (1970) reports that as a plant becomes water stressed or starts to senesce the cell walls of the mesophyll layer cells will break down and deteriorate. Receding water from the cell wall surfaces into the micrifibrillar network will increase leaf reflectance up until the point cell walls deteriorate and no longer reflect. This study showed that the deterioration of cell walls has a greater affect on infrared leaf reflectance that the reduction of air volume in the spongy mesophyll as previously presumed. The presumption

behind this theory is that as plants become stressed, near-infrared reflectance decreases as a function of cell wall deterioration.

A water vapor band absorption band is present from 920-980nm in the near infrared portion of the spectrum, consequently the optimal wavelengths for this spectrum are between 740 -900nm (Tucker, 1979).

3. The middle-infrared wavelengths from 1,300-2,600 nm are used to measure the amount of water in a plant leaf. Within this spectrum there are three water absorption bands at 1,430, 1,940 and 2,600 nm, with the strongest at 2,600nm (Sinclair et al., 1971). Water is a good absorber of middle infrared energy with strong absorption peaks at 1,600 and 2,200 nm. As water potential in the leaves increases and the leaves become more turgid the middle-infrared reflectance decreases. Conversely as leaf water potential declines and leaves become less turgid, middle-infrared reflectance increases (Jensen, 2005). It is interesting to note that the Landsat satellites collect data from two regions in the middle-infrared: band 5 (1,550-1,750 nm) and band 7 (2,080-2,350 nm). These bands were designed to monitor leaf water content.

Gates et al. (1965) summed the light interactions with leaves best using this statement: “Plants absorb efficiently where they require the energy [in the visible for photosynthesis], absorb poorly in the near infrared to keep form becoming overheated and absorb in the middle-infrared in order to be efficient radiators”.

Light Interactions with Crop Canopies

The interaction of solar energy is different between a single leaf and a plant canopy. Plant canopies have a lower percentage of reflectance due to variations in leaf illumination angle, leaf orientation, bidirectional scattering (Figure 6) and non-foliage background such as soil. Knipling (1970) reports that the visible reflectance of a continuous crop canopy is between 3-5% where as a single leaf is around 10%. The infrared reflectance in a continuous crop canopy is 35% where as a single leaf is 50%. The differences between a single leaf and a continuous crop canopy for visible and infrared are about 40% and 70% respectively. The lower reduction in the infrared reflectance of a crop canopy is due to leaf additive reflectance which enhances reflectance.

Shea et al. (1991) conducted a study to determine the canopy reflectance differences of abaxial (underside) and adaxial (upperside) leaf surfaces for corn (*Zea mays*, L.) and soybeans (*Glycine max*., Merr). The results for soybeans in this study showed that reflectance and transmittance in the visible spectrum, especially for green wavelengths, decreased as leaflets approached full expansion, while near-infrared reflectance increased. This showed that leaf pigments developed in conjunction with mesophyll cell enlargement which in turn increased adsorption. As the leaves reached full expansion, reflectance and transmittance increased in the visible spectrum as a result of chlorophyll degradation while near-infrared reflectance remained constant. The results also showed that near-infrared reflected more in the adaxial (upperside) surface and transmitted more on the abaxial (underside) surface while the visible spectrum reflected and transmitted more in the abaxial (underside) surface by approximately 5%.

Other important factors to consider when measuring crop canopy reflectance are leaf hemispherical reflectance, leaf area, leaf orientation, interaction with supporting structures such as stalks, background reflectance, solar zenith angle, look angle and azimuth angle (Colwell, 1974; Knipling, 1970; Thomas and Gausman, 1976).

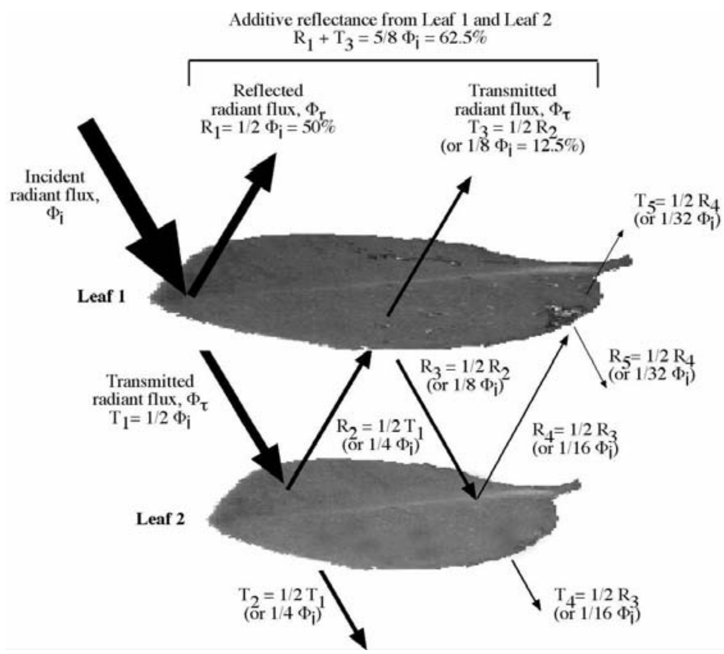

Figure 6. Additive leaf reflectance and leaf response to infrared radiation (Jensen 2005)

Light Interaction with Plant Pigments

As PAR strikes the leaf surface it is intercepted by plant pigments in the chloroplasts and used to capture energy for photosynthesis. The plant pigments responsible for photosynthesis are chlorophyll a and chlorophyll b which absorb light in the blue and red portion of the spectrum and reflect light in the green. The absorption response to chlorophyll can be measured and quantified using the absorbance spectrum (Figure 7). Absorption of chlorophyll a is at wavelengths 430nm and 670nm with small responses at 580nm and 630 nm while chlorophyll b is at wavelengths 460nm and 650nm. At 750nm there is no additional absorption by PAR. The lack of chlorophyll absorption in the green band, at approximately 550nm, is what causes green foliage to appear green to our eyes (Jensen, 2005; Chappelle, 1992).

Other plant pigments such as β-carotene, phycoerythin and phycocyanin also absorb in the visible spectrum (Figure 7). β-carotene has a strong absorption in the blue around 450nm, phycoerythin absorbs primarily in the green around 550nm and phycocyanin absorbs in the yellow primarily around 620nm. Because chlorophyll is the primary pigment with the highest concentration it tends to mask out β-carotene, phycoerythin and phycocyanin (Chappelle, 1992). As a result most or the work centered on the chlorophyll absorption is focused on the wavelengths between 450-520nm and 630-690nm (Thomas and Gausman, 1976; Jensen, 2005).

The “red edge” is the portion of the electromagnetic spectrum between 680 and 750 nm that is related to leaf chlorophyll content. This portion of the spectrum is useful because it represents the high internal leaf reflectance in the near-infrared and the chlorophyll absorption in the red which causes low reflectance. As a result the red edge measurements are useful in determining crop stress as a function of chlorophyll content and leaf area index independent of ground cover. The mechanics of the red edge are based primarily on leaf chlorophyll content; as the chlorophyll content increases the red edge shifts progressively to longer wavelengths. Conversely as chlorophyll content decreases there is a shift in the red edge to shorter wavelengths with an increase in reflection in the green (Curran et al., 1991 and Horler at al., 1983).

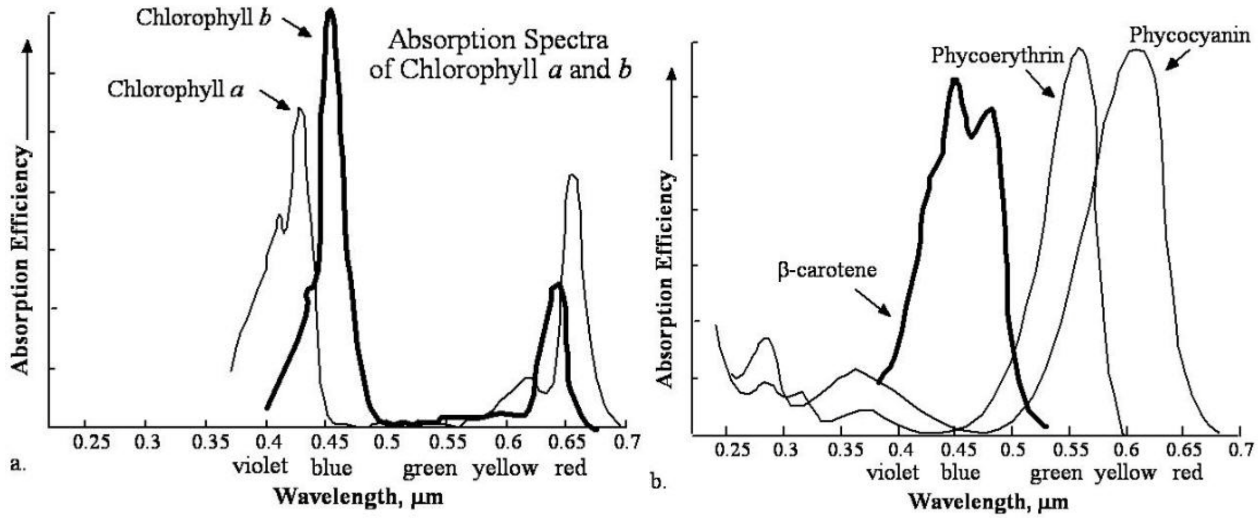

Figure 7. a) Inflection points for chlorophyll a and b, and b) inflection points for β-carotene, phycoerythin and phycocyanin. (Jensen, 2005)

Light Interaction with Soil

Measuring soils using remote sensing is complicated by soil properties such as organic matter, inorganic solids, texture and water content. As a general rule soil reflection is fairly low in the blue channel, but increases somewhat linearly through the red and near-infrared regions of the electromagnetic spectrum (Figure 1). Organic matter, soil water content and surface roughness can affect soil reflectance in the following way: as organic matter and soil water content increases (Bausch, 1993), soils become darker in color which results in a decrease in reflectance. In the same way, as soil roughness increases, for example from tillage practices, reflectance also decreases as a result of increased scattering and shadowing (Rondeaux, 1996).

Vegetative Indices

Vegetation indices have been developed to reduce multi-band observations into a single dimensionless radiometric number in order to enhance green vegetation while normalizing the effects of soil and variations in atmospheric conditions (Jensen, 2005; Wiegand and Richardson, 1990; Wiegand et al., 1991). Vegetation indices are divided into three categories based on their function. The first are the intrinsic or ratio indices, such as the ratio vegetation index (RVI) and the normalized difference vegetation index (NDVI), which are derived as combinations of the red (600-700nm) and near-infrared (700-1300 nm) portions of the spectrum where leaves absorb and reflect energy. These ratios are displayed graphically as two-dimensional lines with an increasing slope diverging out of an origin (Figure 8). These indices are used to enhance the contrast between vegetation and soil particularly when monitoring global vegetative changes (Baret and Guyot, 1991). These indices are related to the biophysical properties of leaves such as photosynthetically active radiation, leaf area index, canopy cover, total chlorophyll and work well until saturation at full canopy. The one disadvantage of these indices is their sensitivity to soil optical properties which make then difficult to interpret with low vegetative cover (Rondeaux, 1996). The second category is the orthogonal indices or “soil line” indices such as the perpendicular vegetation index (PVI), weighted difference vegetation index (WDVI) and the green vegetation index (GVI). These indices are different from the ratio indices in that the greenness lines don’t converge on an origin, but instead remain parallel to a predefined axis that accounts for soil effects, known as the “soil line” (Figure 8). As a result, the soil background remains constant while the green vegetation is expressed (Baret and Guyot, 1991; Chehbouni et al., 1994; Huete et al., 1985). The third category is the atmospherically corrected indices which introduce the blue channel to reduce atmospheric affects. The blue channel can be added in combination with the red channel such as the NDVI in order to create the atmospherically resistant vegetative index (ARVI) with the following formula: ARVI = (NIR-RB)/ (NIR+RB) (Kaufman and Tanré, 1992). This same process can also be applied to the SAVI and the TSAVI by changing the G to GB in the index (Rondeaux, 1996). The disadvantage of this process is that these indices minimize the soil and atmospheric effects independently, but fail to correct for these variables when applied simultaneously (Myeni and Asrar, 1994).

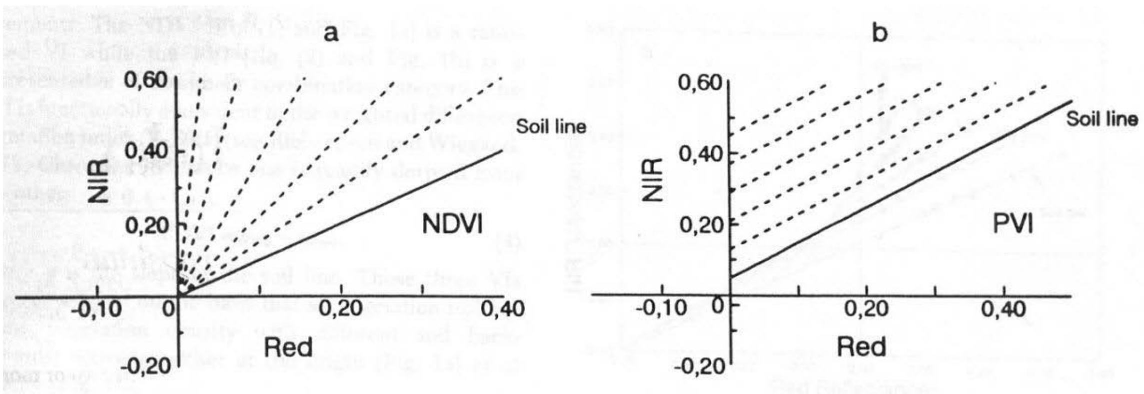

Figure 8. a) NDVI two dimensional soil line diverging our of origin and b) PVI parallel soil line. (Chehbouni et al., 1994)

Vegetative indices were first reported by Jordan (1969) who used a ratio vegetation index (RVI) to measure differences in forest canopies. In 1973 Rouse et al., conducted a study to develop a quantitative measurement for aboveground biomass in rangelands. Bands 5 and 7 from ERTS-1 were recorded and used to develop what is know today as the normalized difference vegetation index (NDVI). Additional research was conducted by Tucker (1979) using linear combinations of the red-infrared bands and red-green bands to quantify differences in plant biomass, leaf water content and chlorophyll content. The combinations of red and infrared bands were compared to the combinations of red and green bands. The results of these comparisons showed that the red-infrared combinations, especially the NDVI, were more significant in showing differences between dry, biomass, wet biomass, leaf water content and total chlorophyll than the red-green combinations. From this study additional red-infrared band combinations, most notably the difference vegetation index (DVI) and ratio vegetation index (RVI), were developed that were consistent in function with the NDVI. In 1996 Gitelson et al. studied the feasibility of indices using the simulated green channel (550nm) of the EOS-MODIS satellite. A new indice, called the green normalized difference vegetation index (GNDVI), was developed based on the NDVI, in which the red band was replaced by the green band. The results of this study showed that GNDVI exhibited a greater sensitivity to chlorophyll concentrations than the NDVI and produced more accurate measurements of pigment concentrations.

The red-infrared indices correlate well with foliage density, as a function of biomass, but remains sensitive to soil background and atmospheric affects (Rondeaux et al., 1996). In an attempt to minimize these effects Huete (1988) developed the soil adjusted vegetation index (SAVI) by modifying the NDVI indice. A soil-adjustment factor *L* was added to account for the first-order soil background. There is an inverse relationship between the *L* factor and vegetation density and can be adjusted based on the following canopy characteristics: A factor of L = 1.0 is applied to low densities while a factor of L = 0.5 and L = 0.25 are applied to intermediate and high densities respectively. An adjustment factor of L=0.5 is the standard since it is normally larger that the red reflectance values and would still buffer soil reflectance variations. The SAVI was modified by Qi et al. (1994) resulting in a new index called the modified soil adjusted vegetation index (MSAVI) which is said to be an improvement over the SAVI in that it replaces the constant variable *L* function with a variable *L* function that accounts for variation between soils and the range of vegetation cover from a very sparse to a very dense canopy. Clevers (1988) developed the weighted difference vegetation index (WDVI), to measure leaf area index and correct for soil background. This model was developed for specific situations where the bare soil ratios of red and near-infrared reflectance remained constant independent of soil moisture. The corrected near-infrared reflectance could then be used as a weighted difference between the measured red and near infrared reflectance.

Crop Growth and Development

Measuring Plant Biomass Differences

Numerous studies have been conducted in the past three decades to develop applications for vegetation indices as well as develop new indices. Most of these vegetation indices focus on the characteristics of crop canopies such as leaf area index, plant density, photosynthetically active biomass, chlorophyll content, wet and dry biomass, plant height, plant populations and yield (Baret and Guyot, 1990; Clevers, 1989; Jones and Holshouser, 2001; Purevdorj, 1998; Senay et al., 2000; Thenkabail et al., 1992; Thenkabail et al., 1994a, Thenkabail et al., 1994b; Tucker, (1979); Wiegand et al., 1990; Wiegand et al. 1991a; Wiegand et al. 1991b).

Tucker (1979) was one of the first to study the relationships of red-infrared band combinations for measuring crop canopy characteristics. The results of this research showed that normalized difference vegetation index (NDVI), transformed normalized vegetation index (TNDVI), square root of the ratio vegetation index (SQRT RVI) and ratio index (RVI) were all very similar in their sensitivity to green leaf area and green leaf biomass.

Purevdorj (1998) conducted a study to examine the relationships between vegetative cover and vegetation indices for grassland in Japan and Mongolia. The results from this study showed that TSAVI, SAVI and MSAVI were significantly better in reducing soil brightness errors than the NDVI but all showed high R^2 correlations, 0.92, 0.89, 0.89 and 0.92 respectively to vegetative cover for all measurements. In other words as the vegetation cover increased, vegetation index values increased.

Senay et al. (2000) conducted a research project to evaluate the ability of a twelve band multi-spectral scanner to identify corn and soybeans at various crop stages. The sensor was configured to collect three blue bands (380-420nm, 420-450nm and 450-500nm), two green bands (500-550nm and 550-600nm), two red bands (600-650nm and 650-690nm), three near-infrared bands (700-790nm, 800-890nm and 920-1,100nm) and two identical middle-infrared bands (1550-1750nm). Three vegetation indices (SVI, NDVI and ND) were developed using band combinations in the red, near-infrared and mid-infrared. The results from this study showed that spectral separation between corn and soybeans was possible using the near-infrared bands at crop maturity, where as the visible bands were useful for soybeans at or before senescence. Differentiation between the spectral classes, three for each crop, were related to leaf nitrogen, soil water, soil carbon and plant biomass. While there were little statistical differences between plant biomass and spectral classes, there was still a strong correlation between the two indicating a positive response of spectral response to increasing biomass.

Studies by Thenkabail et al. (1994b) using Landsat-5 TM data were done to develop and evaluate models that could be used to determine crop yield, leaf area index, wet biomass, dry biomass and plant height for soybeans and corn. Three groups of models were evaluated: linear combinations of TM bands, linear combinations of vegetation indices and logarithmic, exponential and power vegetation indices. Group one models were made from linear combinations of band 2 (green, 520-600nm),band 4 (near-infrared, 760-900nm), band 5 (middle-infrared, 1550-1750nm) and band 7 (Thermal, 2080-2350nm). Group two models were made using near-infrared and red combinations while group three models were exponential and logarithmic models based on trends in the data. The results from this study showed that the best soybean models were from combinations of band 3 (red, 630-690nm) and band 4 (near-infrared, 760-900nm) explaining 69 to 76 percent of the variability from wet biomass, dry biomass and plant height. Leaf Area Index (LAI) was next with 63 percent of the variability followed by yield with 35 percent of the variability. The best corn models were combinations of band 4, 5 and 7. Models for wet biomass were the best, accounting for 80 percent of the variability followed by dry biomass, plant height, LAI and yield with 66 to 67 and 52 percent of the variability respectively. The LAI, which is the most frequently quantified crop growth variable, did not correlate as well as wet and dry biomass and leaf height.

Additional studies by Thenkabail et al. (1992 and1994a) using the same Landsat-5 TM dataset were analyzed to determine the impact of cultural and management practices on soybean and corn as well as evaluate the effect of ground truth data on this process. Crop management practices such as planting date, tillage, soil association, drainage, plant density and stress were studied in relation ship to the following ground truth dataset based on crop attributes: leaf area index, wet biomass, dry biomass and grain yield. Normalized difference vegetative index (NDVI), simple vegetative index (SVI), stress vegetation index 1 (STV1), stress vegetation index 2 (STV2), mid-infrared simple vegetation index one (MSVI1) and mid-infrared simple vegetation index two (MSVI2) were chosen to evaluate crop attributes based on their sensitivity to chlorophyll and biomass differences and well as their ability to minimize soil background reflectance. The results from these studies showed that the best vegetative index or band correlating to soybean yield was TM band 4 with an R^2 of 0.35. Leaf area index, wet biomass and dry biomass all showed the best correlation to NDVI with R^2s of 77, 70 and 70 respectively. The data also showed positive responses to seeding rates in both corn and soybeans. As seeding rates increased the leaf area, wet biomass and dry biomass also increased. These increases were measured quantitatively using vegetative indices.

Jones and Holshouser (2001) conducted research to study the effects of seeding rates on leaf area index. Two soybean varieties (a mid-group III, indeterminate and mid-group V determinate) were tested with varying seeding rates ranging from 123, 000 to 618, 000 plants/hectare in 2000 and 148,000 to 815,000 plants/hectare in 2001. Leaf area measurements were measured multiple times in 2000 and 2001. The results showed that leaf area increased with plant population density for both varieties. The leaf area in the mid-group III started to decline at the R5 developmental stage but remained strong through the early R6 stage for the mid-group V. Color infrared imagery was collected on three different dates in 2001 to test if NDVI could be used to determine differences in leaf area index and yield as a function of seeding rates. The image dates tested corresponded to the flowering, pod development and seed development stages. The results showed that images taken at the pod development stage (R3-R4) had the highest NDVI correlation to leaf are index and yield with R^2 values or 0.84 and 0.96 respectively.

Materials and Methods

Plot Establishment

Field studies were conducted at different sites on the Purdue Agronomy Center for Research and Education (ACRE) near West Lafayette, Indiana in 1994, 1995 and 1996 and at the Throckmorton-Purdue Agricultural Center (TPAC) near Romney, Indiana in 1994. The ACRE sites for all years were within 1,000 meters of one another. Field preparation at both locations consisted of conventional tillage prior to planting.

Treatments

A complete randomized split-block experimental design with four replications was used for each site (Figure 9).

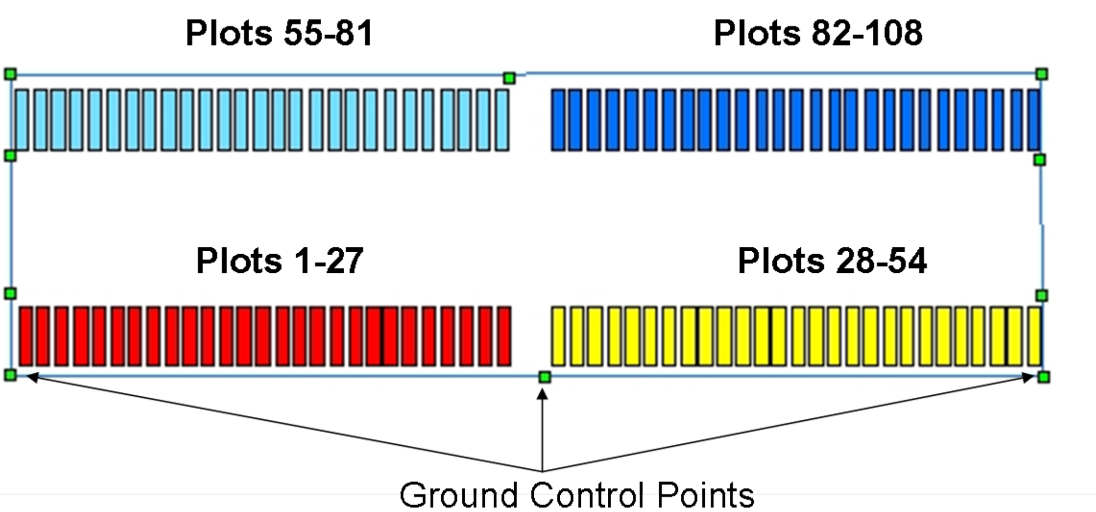

Figure 9. Plot diagram

The main plots were three row spacing treatments: 19cm, 38cm and 76cm. Subplots were nine plant population density treatments with targeting seeding rates ranging from 0 to 988,400 plants ha^{-1} in increments of 123, 550 plants ha^{-1}.

Planting dates for each site was June 6 with the exception of ACRE 2005 which was planted on May 13th. Harvest dates for each site ranged from September 26 to November 3rd. The 19cm rows were planted using 2.07 meter Great Plaines (Great Plains Manufacturing, Salina, KS) drill outfitted with a Hege 80 (Wintersteiger, Des Moines, IA) cone seeding unit. All seed for these plots were weighed prior to planting. The 38cm and 76cm rows were planted using a 6 row John Deere Max Emerge™ (John Deere, Moline, IL) planter with row splitters and a GreenStar™ (John Deere, Moline, IL) adjustable rate seeding controller. Each plot was 4.5 meters wide, representing the planter width, by 22.9 meters long. Plots seeded with the drill required two passes.

A single Dekalb Roundup Ready (DKC 38-52) variety was planted at each site. This variety represented a growth maturity rating of 3.8 which is typical for this geography. A zero seeding rate was used to account for soil effects in the analysis. Roundup® (Monsanto Company, St. Louis, MO) was applied at the label rate of 2.3 l/ha at least twice per season across years and locations. In 2005 Firstrate® (Dow AgroSciences, Indianapolis, IN) was applied once at 43.77 ml/ha to control Ivyleaf Morningglory (*Ipomoea hederacea*). All plots, including the zero seeding, were maintained weed free throughout the growing season to eliminate the effect of weeds in the canopy reflectance.

Data Collection

Ground control targets were placed at the four corners and replication breaks of each site. A Trimble Ag-132 (Trimble Navigation Limited, Sunnyvale, CA) differential global positioning system (dGPS), rated for sub-meter accuracy, was used to collect coordinates at the center of each target and used to geometrically correct each image. Color infrared images (CIR) were collected at each site starting at the V2 growth stage growth stage (Pederson, 2004) and extending through the R7 growth stage with temporal resolution of one week (Table 2). Images were collected between 10 am and 2 pm CST under as cloud free conditions as possible (Appendix Figures 13-39).

Table 2. Image Collection Dates with Corresponding Growth Stages

	TPAC 04	ACRE 04	ACRE05	ACRE 06
Growth Stage	------------------------------	Date	------------------------------	
V2	7/1/2004	7/1/2004	-	6/29/2006
V3	-	-	-	7/7/06
V6	-	-	6/29/2005	-
V7	-	-	-	7/15/2006
R1	7/22/2004	7/22/2004	7/7/2005	7/24/2006
R2	-	-	7/19/05	7/30/06
R3	8/3/2004	8/3/2004	7/29/2005	8/4/2006
R4	8/16/2004	8/16/2004	8/3/2005	8/22/2006
R5	8/30/2004	8/30/2004	8/21/2005	-
R6	9/7/2004	9/7/2004	-	9/15/2006
R7	9/22/2004	9/22/2004	-	-

The images were collected using a Duncantech 4100 (Geospatial Systems Rochester, NY) multi-spectral frame grabber sensor using a belly mounted platform. The sensor was configured to collect in the NIR, red and green portion of the electromagnetic spectrum (500-900 nm). The band configurations for this sensor exhibited very little overlap in order to approximate the Landsat satellite bands (Figure 10).

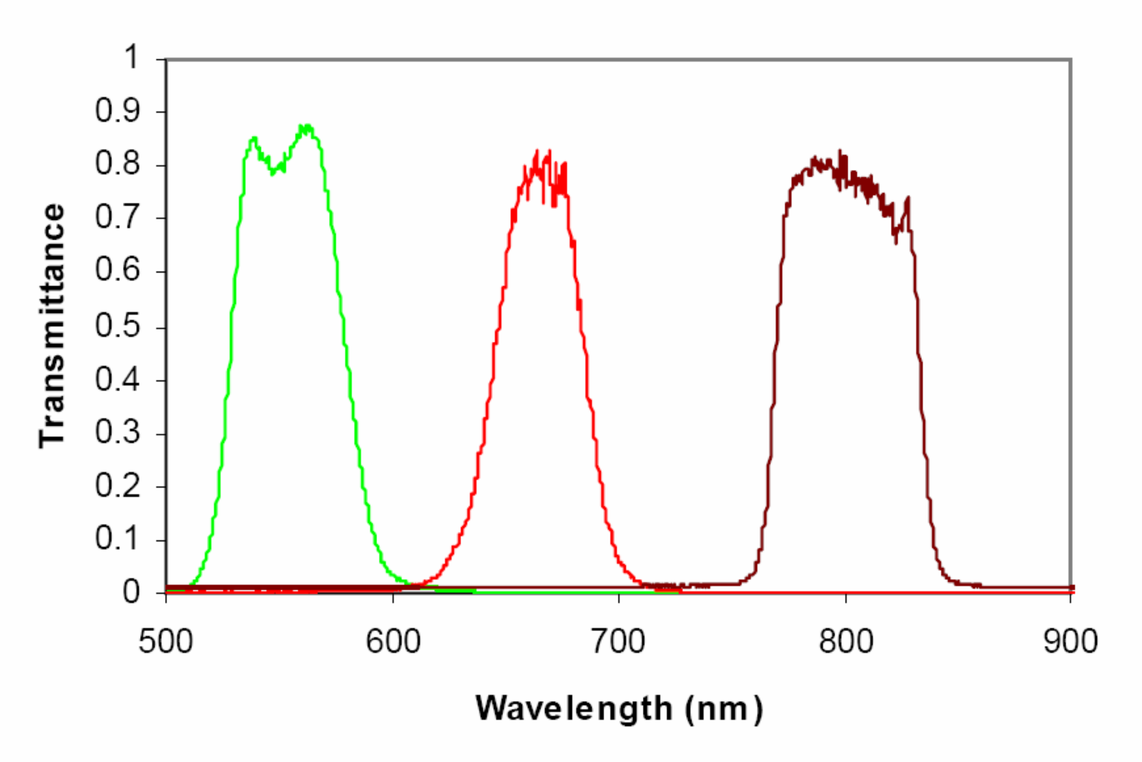

Figure 10. Spectral bands approximating Landsat TM7 for Duncantech 4100 multi-spectral camera

The radiometric resolution of each image was 8-bit, with pixel brightness values ranging from 0-255. Band 1 (NIR) was configured with a center wave length (CWL) of 796 ± 4 nm covering the wavelengths from 766 ± 4 nm to 826 ± 4 nm with a full width at half maximum (FWHM) of 60 ± 8 nm, Band 2 (Red) was configured with CWL of 667.5 ± nm covering the wavelengths from 647.5 ± 2.5 nm to 687.5 ± 2.5 nm with a FWHM of 40 ± 5 nm, Band 3 (Green) was configured with a CWL of 547.5 ± 2.5 nm covering the wavelengths from 527.5 ± 2.5 nm to 567.5 ± 2.5 nm with a FWHM of 40 ± 5 nm (Table 3).

Table 3. Duncantech 4100 Band Configuration

	Band 1 (NIR)	Band 2 (Red)	Band 3 (Green)
CWL	796 ± 4 nm	667.5 ± 2.5 nm	547 ± 2.5 nm
FWFM	60 ± 8nm	40 ± 5 nm	40 ± 5 nm
Cut-On	766 ± 4 nm	647.5 ± 2.5 nm	527.5 ± 2.5 nm
Cut-Off	826 ± 4 nm	687 ± 2.5 nm	567 ± 2.5 nm

The aerial images were collected at an altitude of 450 ± 25 meters in order to achieve a target ground pixel resolution of 30.5 cm or less (Table 4) and to assure that each image encompassed the entire study area. Variations in resolution were the result of altitude differences when the images were collected.

Table 4. Image Resolution by Growth Stage and Site

	ACRE 2004	ACRE 2005	ACRE 2006	TPAC 2004
Growth Stage	----------------------------------Resolution (cm)------------------------------			
V2	18.44	na	na	36.65
V3	na	na	na	na
V7	na	na	33.22	na
V8	na	NA	na	na
R1	24.70	10.33	25.40	27.89
R2	na	8.94	32.77	na
R3	24.03	9.48	27.38	27.16
R4	26.20	na	29.31	35.65
R5	23.96	10.35	na	34.90
R6	28.51	na	na	39.95

Soybean plant population counts were taken in each plot twice throughout the growing season, once at flowering (R1-R2) and at maturity (R7-R8). The 19 and 38 cm row spacing were measured using a 71.1 cm hoop with a multiplier of 25,204 to calculate number of seeds per ha. The 76 cm rows were measured per meter of linear row using a measurement of 5.31 m and a multiplier of 2471 to calculate seeding rate per ha. The average seeding rate from both counts was used in data analysis.

Soybean grain was harvested from the center 1.5 meters of each plot using both an ALMACO HP 5 (ALMACO, Nevada, IA) and Kincaid-8 XP (Kincaid Equipment Manufacturing, Haven, KS) plot combine. Plot lengths ranged from 18.5 to 21.3 meters in length. Grain data was weighed and converted to dry yield (kg/ha) and moisture.

Image Processing

Images were geometrically corrected using Georeferencer (Delta Data Systems, Picayune, MS) with a RMS error ± 1 meter. The dGPS coordinates were used to perform an image-to-point registration on a base image from each site. At all sites the base image was selected from an image collected at or before the R1 growth stage in order to minimize to effects of plant vegetation on the ground targets. The base image from each site was then used in an image-to-image correction for the rest of the images collected at the site. The base images selected for ACRE 2004 and TPAC 2004 were taken on July 1 while ACRE 2005 and ACRE 2006 were taken on July 7 and July 15 respectively. For ACRE 2004 and TPAC 2004 ten ground control targets were placed at each site with a second order polynomial fit to each image and for ACRE 2005 and ACRE 2006 six ground control targets were used with a first order polynomial fit.

Areas of interest (AOI) of equal size (3m by 14.8m) and pixel number were created for each plot using AGIS software (Delta Data Systems, Picayune,MS). The AOIs were used to extract the mean digital number (DN) from each plot for all three spectral bands and calculate multiple vegetative indices (Table 5).

Table 5. Spectral bands and vegetative indices

Vegetative Index	Short Name	Formula*	Reference
Normalized NIR	Norm NIR	NIR/(NIR+R+G)	Sripada et al., 2005
Normalized Red	Norm R	R/(NIR+R+G)	Sripada et al., 2005
Normalized Green	Norm G	G/(NIR+R+G)	Sripada et al., 2005
Simple Ratio	SR	R/NIR	Birth and McVey, 1968
Difference Vegetation Index	DVI	NIR-R	
Green Difference Vegetation Index	GDVI	NIR-G	
Ratio Vegetation Index	RVI	NIR/R	
Green Ratio Vegetation Index	GRVI	NIR/G	
Normalized Difference Vegetation Index	NDVI	(NIR-R)/(NIR+R)	Rouse et al., 1974
Green Normalized Difference Vegetation Index	GNDVI	(NIR-G)/(NIR+G)	
Soil Adjusted Vegetation Index	SAVI	[(NIR-R)/(NIR+R+0.5)]*1.5	Huete, 1988
Green Soil Adjusted Vegetation Index	GSAVI	[(NIR-G)/(NIR+G+0.5)]*1.5	
Optimized Soil Adjusted Vegetation Index	OSAVI	(NIR-R)/(NIR+R+0.16)	Rondeaux et al.,1996
Green Optimized Soil Adjusted Vegetation Index	GOSAVI	(NIR-G)/(NIR+G+0.16)	

* NIR, near infrared; R, red; G, green

Statistical Analysis

The NIR, R and G spectral bands and vegetative indices were regressed against the average soybean seeding rate using the PROC REG function in SAS 9.1 (SAS Institute, Inc., Cary, NC USA 2002-2003). The following regression models were tested: linear, quadratic and polynomial (denoted by X, XX and X_XX respectively). The R^2 and Probability F-values were used to determine the best model and indices for three different analyses: Analysis one was used to test all possible indice and model combinations by site. These results were pooled and the model significance, Probability F and R^2 values were used to determine the optimum soybean growth stage. This information was then used to select the best model and indice by treatment. Analysis two was used determine the best indice and model for each treatment by combining sites. Analysis three determined the best overall model and indice by combining sites and treatments. The results for all three analyses were sorted by probability F-values and included the model significance for both a 95 and 99% confidence level.

Plant population counts were divided by 1000 to reduce numeric differential between the large plant population numbers and the small numbers of the indices. Consequently the regression results for the estimated intercept (β_0), estimated X ($\beta_1 X$) and estimated XX ($\beta_2 X^2$) values are reported in like fashion. These numbers must be multiplied by 1000 before that are applied in an equation.

Results and Discussion

Seeding Rates

The stand count measurements recorded at flowering (R1-R2) and maturity (R7-R8) were averaged together to determine if the target plant populations were reached. The results from the 19cm treatments (Table 6) show that seeding rates, excluding zero, for TPAC 2004 ranged from 138,623 to 872,695 plants ha^{-1}. The seeding rates for ACRE 2004, ACRE 2005 and ACRE 2006 ranged from 201,634 to 948,308 seeds ha^{-1}, 113,365 to 791,564 seeds ha^{-1}and 94,516 to 585,998 seeds ha^{-1}respectively. The plant population to target seeding rate accuracy was best for ACRE 2004 followed by TPAC 2004, ACRE 2005 and ACRE 2006 (Figure 10). The lower than expected plant populations for ACRE 2006 was a result of a seed weighing error prior to planting.

Table 6. Target seeding rates and plant population counts for 19cm treatments

		TPAC 2004	ACRE 2004	ACRE 2005	ACRE 2006
Treatment	Target Rate	-------------------Plant population seeds ha^{-1} -------------------			
1	0	0	0	0	0
2	123,550	138,623	201,634	113,365	94,516
3	247,100	259,918	261,494	204,068	157,526
4	370,650	382,789	419,020	320,970	201,634
5	494,200	452,888	585,998	396,031	258,343
6	617,750	568,670	639,557	497,180	289,848
7	741,300	657,672	727,771	644,041	384,364
8	864,850	778,180	841,190	664,050	447,375
9	988,400	872,695	948,308	791,564	585,998

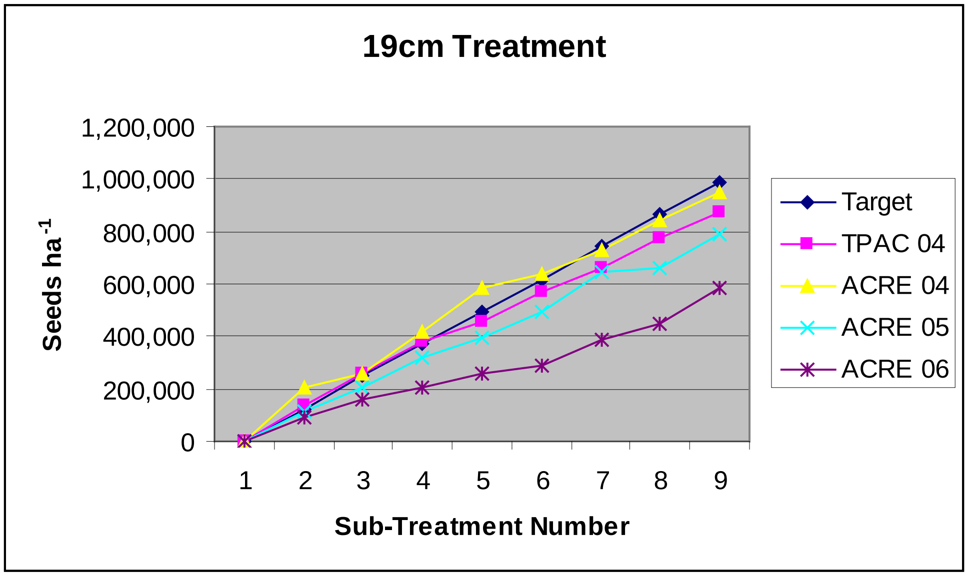

Figure 10. Comparison of target seeding rates to plant population counts by site for 19cm treatments

The results from the 38cm treatments (Table 7) show that seeding rates, excluding zero, for TPAC 2004 ranged from 256,768 to 992,415 plants ha^{-1}. The seeding rates for ACRE 2004, ACRE 2005 and ACRE 2006 ranged from 269,370 to 967,211 seeds ha^{-1}, 211,184 to 887,614 seeds ha^{-1}and 201,634 to 649,008 seeds ha^{-1}respectively. The plant population to target seeding rate accuracy was very similar for TPAC 2004, ACRE 2004 and ACRE 2005 and decreased by as much as 35 % in ACRE 2006 (Figure 11). A target seeding rate of 123,550 was not achievable for 38cm treatments due to the planter's inability to seed at such low rates. The decrease in plant populations for ACRE 2006 was due to operator error and incorrect set-up of the seeding monitor.

Table 7. Target seeding rates and plant population counts for 38cm treatments

Treatment	Target Rate	TPAC 2004	ACRE 2004	ACRE 2005	ACRE 2006
		-------------------Plant population seeds ha^{-1} -------------------			
1	0	0	0	0	0
2	247,100	256,768	269,370	211,184	201,634
3	247,100	264,644	265,432	257,406	195,333
4	370,650	400,117	419,020	374,239	280,397
5	494,200	485,181	488,331	485,904	313,477
6	617,750	615,928	585,998	587,897	428,471
7	741,300	706,505	738,798	701,413	502,509
8	864,850	836,464	838,827	831,153	548,191
9	988,400	992,415	967,211	887,614	649,008

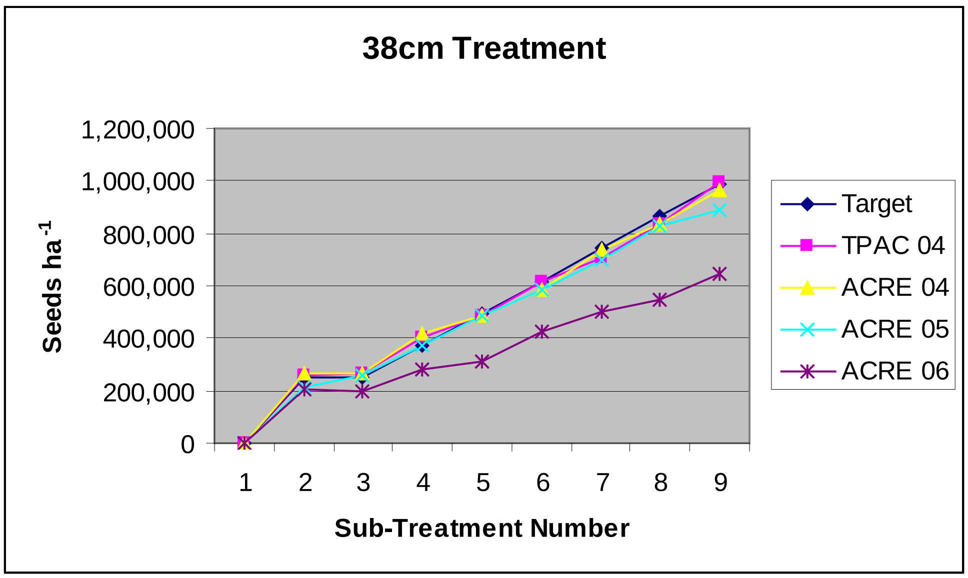

Figure 11. Comparison of target seeding rates to plant population counts by site for 19cm treatments

The results from the 76cm treatments (Table 8) show that seeding rates, excluding zero, for TPAC 2004 ranged from 106,716 to 706,938 plants ha^{-1}. The seeding rates for ACRE 2004, ACRE 2005 and ACRE 2006 ranged from 115,828 to 787,168 seeds ha^{-1}, 129,577 to 878,697 seeds ha^{-1}and 103,602 to 294,589 seeds ha^{-1}respectively.

The plant population to target seeding rate accuracy was very similar for ACRE 2004 and ACRE 2005 and decreased by as much as 57% for TPAC 2004 and 71% for ACRE 2006 (Figure 12). The decrease in plant populations for TPAC 2004 and ACRE 2006 was due to operator error and incorrect set-up of the seeding monitor.

Table 8. Target seeding rates and plant population counts for 76cm treatments

		TPAC 2004	ACRE 2004	ACRE 2005	ACRE 2006
Treatment	Target Rate	Plant population seeds ha^{-1}			
1	0	0	0	0	0
2	123,550	106,716	115,828	120,577	103,602
3	247,100	165,171	219,610	247,518	102,670
4	370,650	220,614	319,917	353,224	145,228
5	494,200	217,525	442,850	440,121	164,862
6	617,750	268,567	548,099	565,253	181,078
7	741,300	322,002	627,171	676,139	235,131
8	864,850	429,722	697,517	821,747	260,355
9	988,400	706,938	787,168	878,697	294,589

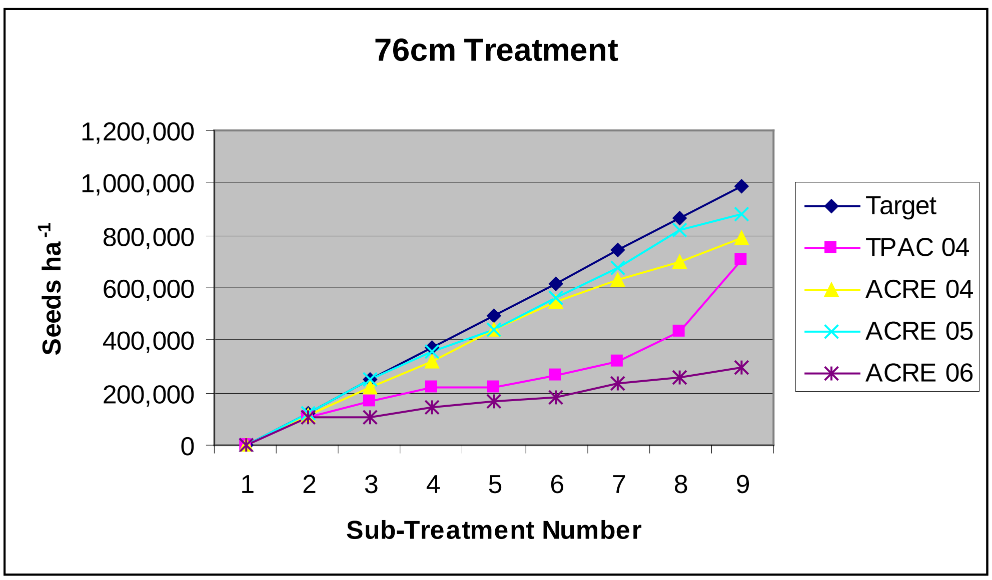

Figure 12. Comparison of target seeding rates to plant population counts by site for 19cm treatments

Spectral Response by Site

A total of 4284 indice and model combinations, 1,071 for TPAC 2004 and ACRE 2004, 918 for ACRE 2005 and 1,224 for ACRE 2006, were pooled together. The model significance, Probability F and R^2 values were used to determine the best indice and model for each site by treatment in addition to identifying the best soybean growth stage for measuring these differences.

The results to test model significance show that 86% of the models tested were highly significant at the 99% confidence level while 5% were significant at the 95% confidence level. The remaining 8% of the models were not significant (Table 9).

There was a direct relationship between model significance and vegetative growth. The number of models that were significance at the 99% confidence level increased from 50 to 95% with increasing vegetation (V2 to V7) while the non-significant models degreased from 43 to 2%. Model significance was greatest during peak vegetative growth (V7-R6), with 88 to 95% of the models showing significance. At the V2 growth stage 43% of the models tested showed no significance while 7 % and 50% showed significance at the 95% and 99% confidence levels respectively. At the V7 growth stage 12% of the models tested showed no significance while 24 % and 65% showed significance at the 95% and 99% confidence levels respectively. The difference between the V2 and R7 growth stages are caused by soil reflectance and leaf senescence respectively. The soil reflectance at the V2 growth stage affects model significance more than the senescing crop canopy at the R7 growth stage.

Model significance is not a good measure of optimum growth stage because 92% of the models tested exhibit some level of positive response to vegetative cover with no differentiation between growth stages.

Table 9. Model significance by growth stage for all sites

Site*	Growth Stage**	No Sig	Sig .05	Sig .01	Total
1,2,4	V2	198(43%)	30 (7%)	231 (50%)	459 (11%)
4	V3	17 (11%)	6 (4%)	130 (85%)	153 (4%)
3	V6	18 (12%)	5 (3%)	130 (85%)	153 (4%)
4	V7	3 (2%)	5 (3%)	145 (95%)	153 (4%)
1,2,3,4	R1	28 (5%)	19 (3%)	565 (92%)	612 (14%)
3,4	R2	16 (5%)	20 (7%)	270 (88%)	306 (7%)
1,2,3,4	R3	22 (4%)	28 (5%)	562 (92%)	612 (14%)
1,2,3,4	R4	22 (4%)	22 (4%)	568 (93%)	612 (14%)
1,2,3	R5	8 (2%)	14 (3%)	437 (95%)	459 (11%)
1,2,4	R6	20 (4%)	8 (2%)	431 (94%)	459 (11%)
1,2	R7	36 (12%)	72 (24%)	198 (65%)	306 (7%)
Total		388 (8%)	229 (5%)	3667 (86%)	4284

* Site codes: 1=TPAC 2004; 2=ACRE 2004; 3=ACRE 2005; 4=ACRE 2006

** Pederson, 2004

In order to analyze the R^2 values they were grouped together by site and treatment and sorted by growth stage and Probability F. The best R^2 values were selected and placed in Tables 10, 11 and 12.

Analyses across row spacing show a strong correlation between R^2 values and the R1 growth stage. In 2004 the R^2 values at both sites were highest for the R1 growth stage. In 2005 the highest R^2 values were at R1 for the 19cm and 76cm treatments and V6 for the 36cm treatment. In 2006 the highest R^2 values were at V3 for the 19cm and 36cm treatments and R3 for the 76cm treatments. The higher than expected results at V3 in 2006 were a result of early vegetative growth and a haze free day when the image was collected. This translated into an image with high radiometric qualities. The decrease in R^2 values at R1 was due to haze in the image resulting in poor radiometric quality that could not be corrected using vegetative indices. The quality of images collected in 2006 was better at earlier growth stages and declined throughout the season. This is a result of camera calibration and set-up and atmospheric conditions.

The results for 19cm treatments are shown in Table 10. The highest R^2 values of 0.93, 0.73and 0.88 correspond to the R1 growth stage for both sites in 2004 and one in 2005. In 2006 the best correlation is at V3. Table 11 shows the results for 36 cm treatments. The best correlation is at R1 for both sites in 2004, V6 in 2005 and V3 in 2006 with R^2 values of 0.87, 0.69, 0.79 and 0.91 respectively. Table 12 shows the results for 76cm treatments. The best correlation is at R1 for three of the four sites. In 2006 the best correlation is at V3.

Comparing the results of model significance in Table 9 to the R^2 values in Tables 10, 11, and 12 show that growth stages R3-R7 have high model significance but decrease in R^2 values as soybeans mature. The decreasing R^2 values in relationship to plant maturity are caused by changes in leaf structure. Shea et al. (1991) reports that as leaves reach full expansion, reflectance and transmittance increase in the visible spectrum as a result of chlorophyll degradation while the near-infrared remains constant. This causes the vegetation indices that use red-near infrared combinations to saturate leading to a reduction in R^2 values.

Table 10. Table of best R^2 by site for 19cm row spacing

Growth Stage	TPAC 2004	ACRE 2004	ACRE 2005	ACRE 2006
		R^2		
V2	0.5972	0.1734	-	0.7974
V3	-	-	-	0.9050
V6	-	-	0.4937	-
V7	-	-	-	0.8243
R1	0.9333	0.7299	0.8780	0.6896
R2	-	-	0.7771	0.8551
R3	0.6699	0.7167	0.4938	0.7898
R4	0.5798	0.5147	0.3742	0.6832
R5	0.4343	0.4756	0.3762	0.4722
R6	0.3697	0.4370	-	-
R7	0.4104	0.4950	-	-

Table 11. Table of best R^2 by site for 36cm row spacing

Growth Stage	TPAC 2004	ACRE 2004	ACRE 2005	ACRE 2006
		R^2		
V2	0.6587	0.2604	-	0.8161
V3	-	-	-	0.9099
V6	-	-	0.7897	-
V7	-	-	-	0.8130
R1	0.8710	0.6893	0.7418	0.5815
R2	-	-	0.5195	0.6214
R3	0.6199	0.5785	0.4408	0.6538
R4	0.5468	0.4678	0.4217	0.4390
R5	0.3994	0.4767	0.4314	0.4670
R6	0.3668	0.5348	-	-
R7	0.3990	0.3603	-	-

Table 12. Table of best R^2 by site for 76cm row spacing

Growth Stage	TPAC 2004	ACRE 2004	ACRE 2005	ACRE 2006
		R^2		
V2	0.5850	0.0779	-	0.5938
V3	-	-	-	0.8187
V6	-	-	0.6243	-
V7	-	-	-	0.7494
R1	0.8084	0.7138	0.7159	0.6674
R2	-	-	0.5573	0.8145
R3	0.7337	0.6381	0.3645	0.8231
R4	0.6580	0.5236	0.3308	0.7254
R5	0.4855	0.4903	0.3629	0.4836
R6	0.4114	0.4782	-	-
R7	0.3097	0.3983	-	-

The results for the best indices and models by site are presented in Appendix Tables 22-33. Data are arranged by site and row spacing treatments with the best of each indice sorted by Probability F values. This data is synthesized in Table 13 which lists the best indice and model for each site by treatment. The results show that the best indices and models for each site and row spacing were identified at the R1 growth stage at three of the four sites. The results for ACRE 2006 identify V7 as the best growth stage for 38cm treatments and R^2 for both 19 and 76cm treatments. These results in Table 13 are consistent with the findings for model significance and R2 analysis listed above.

There was little consistency between indices and models in Table 13. Six different indices were identified in order of frequency: RVI, GRVI, Norm G, GDVI, NIR and GSAVI. The best indice for 19cm treatments is RVI with a quadratic mode and R^2 of 0.93. The best model for 38cm treatments is NIR with a polynomial model and R^2 of 0.87 and the best model for 76cm treatments is RVI with a quadratic model and R^2 of 0.81. The best overall R^2 values were from TPAC 2004.

Table 13. Best indice, model*, R^2 and crop growth stage ** by site

Row Spacing	Best Measure	TPAC 2004	ACRE 2004	ACRE 2005	ACRE 2006
19 cm	Indice:	RVI	RVI	GRVI	GDVI
	Model:	(XX)	(X)	(X_XX)	(XX)
	R^2:	R^2 0.9333	R^2 0.7299	R^2 8780	R^2 0.8551
	Crop Stage:	R1	R1	R1	R2
38 cm	Indice:	NIR	Norm G	GSAVI	GRVI
	Model:	(X_XX)	XX	(X_XX)	(XX)
	R^2:	R^2 0.8710	R^2 0.7138	R^2 0.7418	R^2 0.8130
	Crop Stage:	R1	R1	R1	V7
76 cm	Indice:	RVI	Norm G	GRVI	RVI
	Model:	(XX)	(XX)	(X_XX)	(XX)
	R^2:	R^2 0.8084	R^2 0.7138	R^2 0.7159	R^2 0.8145
	Crop Stage:	R1	R1	R1	R2

* X = Linear; XX = Quadratic; X_XX = Polynomial
** V7 = Seven fully developed trifoliate leaf nodes; R1 = One open flower at any node on the main stem; R2 = One flower at one of the two uppermost nodes on the main stem

Spectral Response by Treatment

The spectral response by treatment was determined by combining sites. A Proc Sort routine in SAS was used to identify the best indice and model by treatment using the crop stages listed in Table 13. Data were sorted by probability F and R^2 values and the results listed in Tables 14, 16 and 16.

Results from all three tables show that the best indice by row spacing is the Normalized Red (Norm R) with a polynomial model. The 19cm treatment has the highest Norm R R^2 value of 0.6982 followed by the 75cm treatment and 36 cm treatment with R^2 values of 0.6369 and 0.5993 respectively. The green band shows the worst correlation for all treatments with R^2 values ranging from 0.0515 in 76cm treatments to 0.1313 in 19cm treatments.

The order of the indices in Tables 14, 15 and 16 can be grouped together based by band combinations. The first eight indices, for each treatment, are those derived from red - near infrared band combinations. These indices are the Red, Norm R, Norm NIR, DVI, RVI, NDVI, and SAVI. The next set of indices is derived from green – near infrared band combinations and is listed as follows: Green, Norm G, GVI, GRVI, GDVI, GSAVI and GOSAVI. The third set is the NIR and SR which is intertwined with the green-near infrared set near the bottom of the tables. The grouping of these indices is consistent with the results of a study done by Tucker (1979) to evaluate and quantify the relationship of red and near infrared combination to plot biomass, water content and chlorophyll content. The results of this study show that red and near-infrared band combinations are sensitive to green leaf biomass and can be used to measure photosynthetically active biomass of plant canopies.

Table 14. Table of best indices by 19 cm row spacing

Name	Model	ProbF	RSq	Mod Sig	EstIntercept	EstX	EstXX
Norm R	X_XX	0.0000000000	0.6982	**	2236.490756	-2747.897507	2026.025946
DVI	X_XX	0.0000000000	0.6706	**	538.905581	2.804556	0.008489
SAVI	X	0.0000000000	0.6539	**	544.161377	276.574713	
NDVI	X	0.0000000000	0.6538	**	544.150548	413.803385	
OSAVI	X	0.0000000000	0.6538	**	544.150019	414.136623	
Red	X_XX	0.0000000000	0.6662	**	1574.529155	-6.780849	0.017903
RVI	X_XX	0.0000000000	0.6564	**	-339.345228	500.586090	-139.112852
Norm IR	X	0.0000000000	0.5179	**	-377.857341	1094.983897	
GRVI	X_XX	0.0000000000	0.4066	**	-924.029368	1028.220305	-428.090324
GVI	XX	0.0000000000	0.3671	**	540.750397		-1720.722737
GOSAVI	XX	0.0000000000	0.3670	**	540.729446		-1724.202938
GSAVI	XX	0.0000000000	0.3668	**	540.682403		-769.498547
GDVI	X_XX	0.0000000000	0.3016	**	509.789968	0.887903	-0.041756
NIR	X	0.0000000002	0.2565	**	-249.233365	3.706537	
SR	X_XX	0.0000011389	0.1835	**	186.740451	166.892652	-54.500805
Norm G	XX	0.0000130175	0.1309	**	31.083113		1412.453165
Green	X_XX	0.0000750203	0.1313	**	-432.480801	9.750307	-0.064238

Table 15. Table of best indices by 36 cm row spacing

Name	Model	ProbF	RSq	Mod Sig	EstIntercept	EstX	EstXX
Norm R	X_XX	0.0000000000	0.5993	**	2385.357143	-3166.393953	2577.361690
SAVI	X	0.0000000000	0.5167	**	512.325125	259.023393	
OSAVI	X	0.0000000000	0.5166	**	512.306020	387.860326	
NDVI	X	0.0000000000	0.5166	**	512.303198	387.549622	
DVI	X_XX	0.0000000000	0.5318	**	505.054552	2.577060	0.007647
RVI	X_XX	0.0000000000	0.5171	**	-324.750105	475.417422	-133.277173
Red	X_XX	0.0000000000	0.4770	**	1317.958718	-5.217778	0.012541
Norm IR	X	0.0000000000	0.3753	**	-296.797417	972.825319	
GRVI	X_XX	0.0000000000	0.3117	**	-794.303088	931.281962	-383.094209
GVI	XX	0.0000000000	0.2819	**	547.211514		-1541.214534
GOSAVI	XX	0.0000000000	0.2818	**	547.190563		-1544.122213
GSAVI	XX	0.0000000000	0.2817	**	547.145088		-689.032983
GDVI	XX	0.0000000147	0.2095	**	517.066650		-0.042221
NIR	X	0.0000000244	0.2038	**	-169.161014	3.333138	
Norm G	XX	0.0000015558	0.1555	**	-8.309406		1639.230810
SR	X_XX	0.0000035401	0.1685	**	180.819517	186.338456	-58.406014
Green	X_XX	0.0000750583	0.1304	**	-430.083089	9.280564	-0.056960

Table 16. Table of best indices by 76 cm row spacing

Name	Model	ProbF	RSq	Mod Sig	EstIntercept	EstX	EstXX
Norm R	X_XX	0.0000000000	0.6369	**	2822.455817	-3824.264101	3183.502711
DVI	X_XX	0.0000000000	0.6368	**	558.150925	3.838607	0.015428
RVI	X	0.0000000000	0.6165	**	-261.296117	331.345632	
SAVI	X_XX	0.0000000000	0.6210	**	567.161262	476.494592	247.426104
OSAVI	X_XX	0.0000000000	0.6210	**	567.161633	713.223124	554.206934
NDVI	X_XX	0.0000000000	0.6210	**	567.175626	712.592947	553.177681
Red	X_XX	0.0000000000	0.5496	**	1555.348690	-6.839917	0.018048
Norm IR	XX	0.0000000000	0.4666	**	-138.247511		2378.154526
GVI	XX	0.0000000000	0.3460	**	422.744743		-1447.654638
GOSAVI	XX	0.0000000000	0.3459	**	422.722829		-1450.458423
GSAVI	XX	0.0000000000	0.3457	**	422.663901		-647.159307
GRVI	X_XX	0.0000000000	0.3489	**	-805.311082	900.046347	-395.746304
NIR	XX	0.0000000070	0.2137	**	12.910193		0.025729
GDVI	XX	0.0000000149	0.2053	**	380.215320		-0.032154
SR	X_XX	0.0000002538	0.1963	**	67.032334	172.707695	-52.796813
Norm G	XX	0.0000021759	0.1485	**	-73.403107		1554.278112
Green	X_XX	0.0253780581	0.0515	*	-14.932848	3.725309	-0.023480

Table 17 lists the R^2 values red- near infrared band combination indices by treatment. The R^2 values in this table show a treatment effect. The 19cm treatment has the highest R^2 values followed by 76cm and 36cm treatments respectively. These values show that the indices and models from 19cm treatments have the best correlation to soybean seeding rates followed by 76cm and 36cm. The reason the 36cm treatments are the lowest may be caused by the moray effect in which the spatial resolution equals the row width.

Table 17. Best R^2 for each indice by row spacing for red and infrared combinations.

	Treatments		
	19cm	36cm	76cm
Indice	----------------------------	R^2	----------------------------
Norm Red	0.70	0.60	0.64
DVI	0.67	0.53	0.64
RVI	0.66	0.52	0.62
NDVI	0.65	0.52	0.62
SAVI	0.65	0.52	0.62
OSAVI	0.65	0.52	0.62
Red	0.67	0.48	0.55
Norm NIR	0.52	0.38	0.47

The R^2 values for the red-near infrared indices in Tables 14, 15 and 16 are very similar. In order to determine differences in R^2 values they were sorted by Probability F values. Consequently there is no consistency in their order across treatments. The R^2 values in Table 17 were sorted independent of the Probability F values in an attempt to determine a trend by order of significance. The data in Table 17 shows Norm R to be the best indice, followed by DVI, RVI. It is interesting to note that NDVI, SAVI and OSAVI have identical R^2 values within treatments and are consistent across treatments. This indicates that at the R1 growth stage the soil adjustment factor in SAVI and OSAVI are no longer needed. The red band and the Norm NIR indice show the lowest R^2 values with in and across treatments with the exception of the Red band in 19cm treatments. The red band in 16cm treatments is comparable to DVI indice, which indicates that the Red band is susceptible to treatment effect.

Table 18 lists the models for the red-near infrared indices by treatment. The data in this table show that the linear and polynomial models work best with the exception of Norm NIR which prefers the quadratic model in 76cm treatments. In the 19cm and 36cm treatments the polynomial model works best the Norm R, DVI, RVI indices and the red band. The linear model works best for the NDVI, SAVI and OSAVI. In the 76cm treatments the polynomial model works best in the Norm R, DVI, NDVI, SAVI, OSAVI indices and the red band. There is one linear model and one quadratic model for the RVI and Norm NIR indices respectively.

Table 18. Best model for each indice by row spacing for red and infrared combinations.

	Treatments		
	19cm	36cm	76cm
Indice	---------------------------Model---------------------------		
Norm Red	X_XX	X_XX	X_XX
DVI	X_XX	X_XX	X_XX
RVI	X_XX	X_XX	X
NDVI	X	X	X_XX
SAVI	X	X	X_XX
OSAVI	X	X	X_XX
Red	X_XX	X_XX	X_XX
Norm NIR	X	X	XX

Spectral Response across Treatments

The best overall model was determined by combining sites and treatments. A Proc Sort routine in SAS was used to identify the best overall model and indice for the complete data set. Data were sorted by Probability F values and listed in Table 19. The results from this analysis are very similar to the results form the spectral response to treatments.

The results from Table 19 show that Norm R is the best overall indice with an R^2 value of 0.6511. The green band also shows the worst correlation with a R^2 value of 0.0851. The order of indices in this table can also be grouped together by band combinations showing identical results to Tables 14, 15 and 16.

Table 19. Table of best indice by combining sites and treatments

Name	Model	ProbF	RSq	Mod Sig	EstIntercept	EstX	EstXX
Norm R	X_XX	0.0000000000	0.6511	**	2295.557414	-2904.101795	2220.594030
DVI	X_XX	0.0000000000	0.6149	**	520.532964	2.907301	0.009628
SAVI	X	0.0000000000	0.5965	**	525.450465	274.965367	
NDVI	X	0.0000000000	0.5965	**	525.456102	411.427284	
OSAVI	X	0.0000000000	0.5965	**	525.450565	411.746167	
RVI	X_XX	0.0000000000	0.6007	**	-346.021553	489.562369	-133.572835
Red	X_XX	0.0000000000	0.5738	**	1474.392685	-6.253316	0.016084
Norm IR	X	0.0000000000	0.4615	**	-391.722610	1089.259346	
GRVI	X_XX	0.0000000000	0.3410	**	-839.743108	944.140391	-393.741240
GVI	X_XX	0.0000000000	0.3270	**	504.610667	81.072700	-1419.002602
GOSAVI	X_XX	0.0000000000	0.3269	**	504.582983	81.119997	-1421.714805
GSAVI	X_XX	0.0000000000	0.3267	**	504.520843	54.156778	-634.357294
NIR	X	0.0000000000	0.2400	**	-265.560732	3.709823	
GDVI	X_XX	0.0000000000	0.2322	**	468.416622	0.786986	-0.031190
SR	X_XX	0.0000000000	0.1703	**	160.899050	166.650518	-53.601951
Norm G	XX	0.0000000000	0.1569	**	-37.176211		1610.469565
Green	X_XX	0.0000000092	0.0851	**	-184.743988	6.380129	-0.040488

Table 20 shows the R^2 values for the red-near infrared band combination indices by treatments (Table 17) and combined treatments. The R^2 values for all treatments are consistent with the 16cm, 36cm and 76cm treatments. The data also confirms that Norm R is the best indice followed by DVI and RVI. The NDVI, SAVI, OSAVI also have identical R^2 values. The Red band and Norm NIR indice show similar results to the 76cm treatment.

Table 20. Best R^2 for each indice by row spacing for red and infrared combinations.

	Row Spacing			
	19cm	36cm	76cm	All Spacing*
Indice	R^2			
Norm Red	0.70	0.60	0.64	0.65
DVI	0.67	0.53	0.64	0.61
RVI	0.66	0.52	0.62	0.60
NDVI	0.65	0.52	0.62	0.60
SAVI	0.65	0.52	0.62	0.60
OSAVI	0.65	0.52	0.62	0.60
Red	0.67	0.48	0.55	0.57
Norm NIR	0.52	0.38	0.47	0.46

* All spacing = 19, 36 and 76cm row spacing combined

Table 21 lists the models for red-near infrared band combinations indices by treatment (Table 18) and combined treatments. The results show that the polynomial model works best for the Norm R, DVI, RVI indices and the Red band. The linear model works best for the NDVI, SAVI, OSAVI and Norm NIR indices. The results for all treatments combines are identical to the 19cm and 36cm treatments.

Table 21. Best R^2 for each indice by row spacing for red and infrared combinations.

	Row Spacing			
	19cm	36cm	76cm	All Treatments*
Indice	Model			
Norm Red	X_XX	X_XX	X_XX	X_XX
DVI	X_XX	X_XX	X_XX	X_XX
RVI	X_XX	X_XX	X	X_XX
NDVI	X	X	X_XX	X
SAVI	X	X	X_XX	X
OSAVI	X	X	X_XX	X
Red	X_XX	X_XX	X_XX	X_XX
Norm NIR	X	X	XX	X

* All treatments = 19, 36 and 76cm treatments combined

Conclusions

This study demonstrated that color infrared imagery is useful for determining differences in soybean seeding rates. Analyses to examine spectral response by treatment and across treatments revealed that the Normalized Red vegetation index and polynomial regression model correlated nicely with soybean seeding rates. Indices developed from red-near infrared band combinations performed consistently better than green- near infrared band combinations. The Norm R vegetation index is a function of the chlorophyll absorption in the red band. As seeding rates increase, plant biomass and red absorption increases. This confirms work done by Tucker (1979) showing that red and near infrared band combinations are useful in quantifying plot biomass, water content and chlorophyll content.

Analyses of model R2 values by growth stage, site and treatment show that seeding rate detection is best at the V7 to R^2 growth stage. Analyses prior to V7 are affected low vegetative cover and soil affects while analysis after R3 is affected by increased red reflectance. Increased red reflectance in proportion to relatively unchanging near infrared reflectance causes the red-near infrared indices to saturate, resulting in a reduction of R^2 values.

The results of this study are consistent with research showing that remote sensing and vegetation indices are useful for determining differences in plant biomass.

References

Kaufman, Y.J., and Tanré D. 1992. Atmospherically resistant vegetation index (ARVI) for EOS-Modis. IEEE Trans. GeoSci. Remote Sens. 30(2):261-270.

Curran, P.J., J.L Dungan, B.A.Macler, and S.E.Plummer. 1991. The effect of a red leaf pigment on the relationship between red edge and chlorophyll concentration. Remote Sens. Environ. 35:69-76.

Moran M.S., Y. Inoue, and E. M. Barnes. 1997. Opportunities and limitations for image-based remote sensing in precision crop management. Remote Sens. Environ. 61:319-346.

Appendices

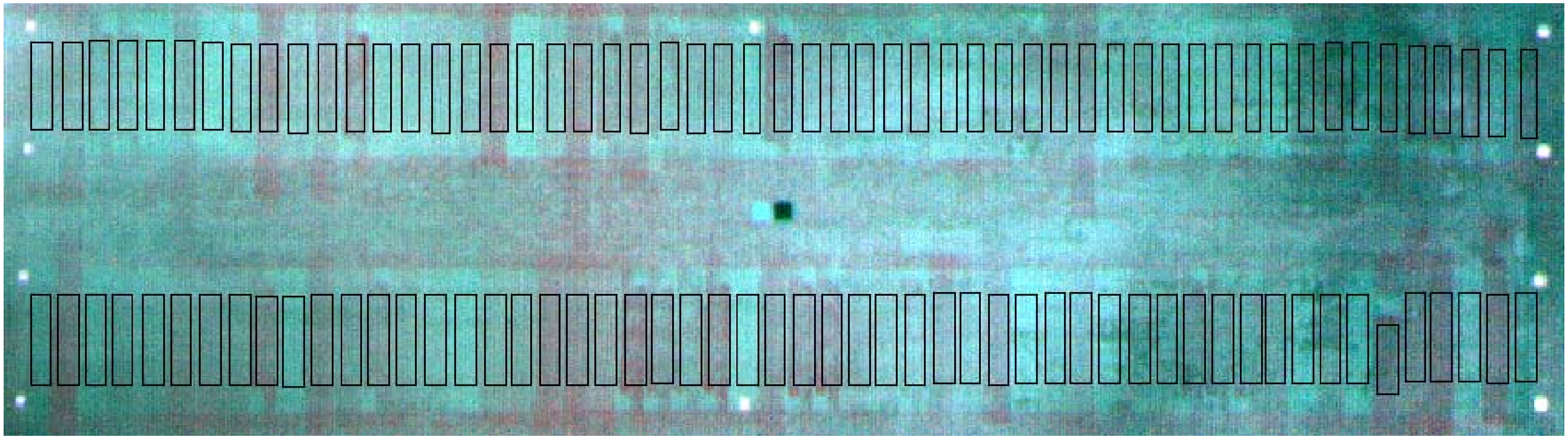

Figure 13. TPAC 2004 - Color infrared image taken July 1, 2004 at the V2 growth stage

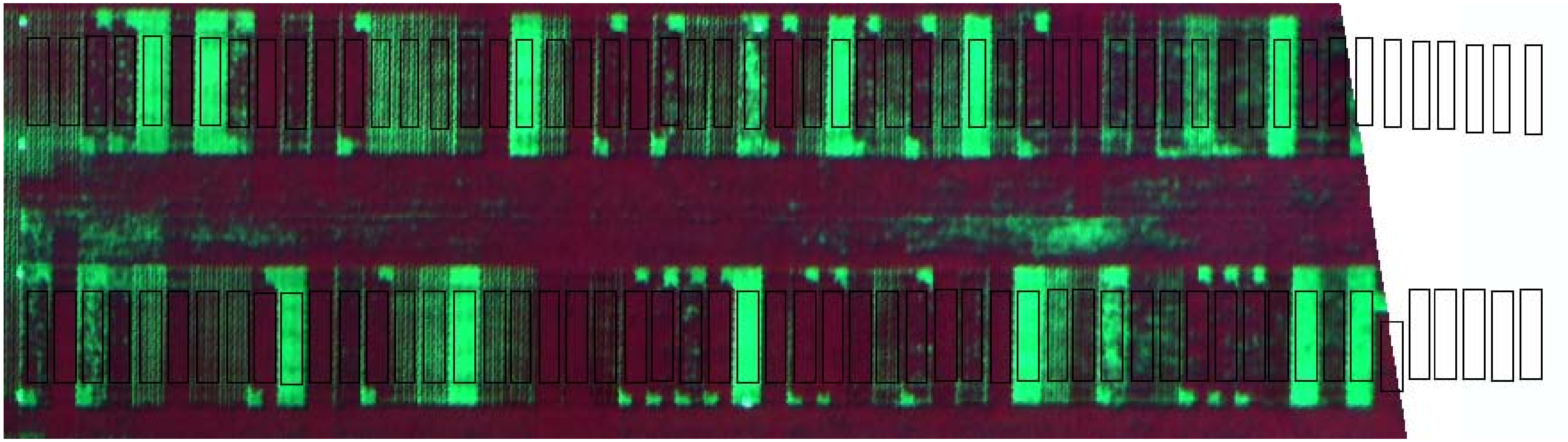

Figure 14. TPAC 2004 - Color infrared image taken July 22, 2004 at the R1 growth stage

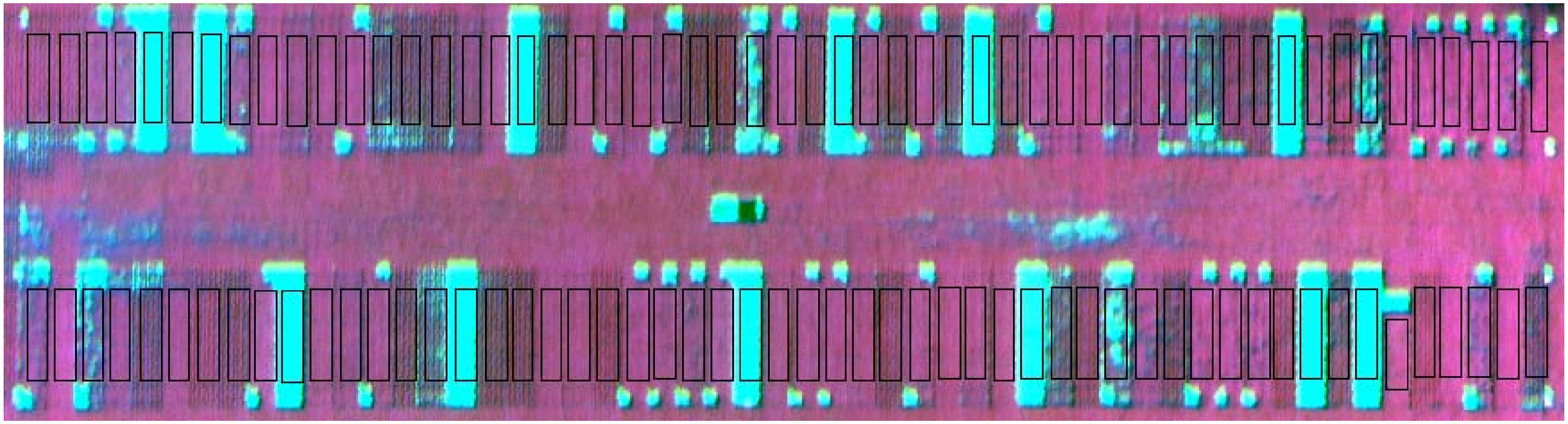

Figure 15. TPAC 2004 - Color infrared image taken August 3, 2004 at the R3 growth stage

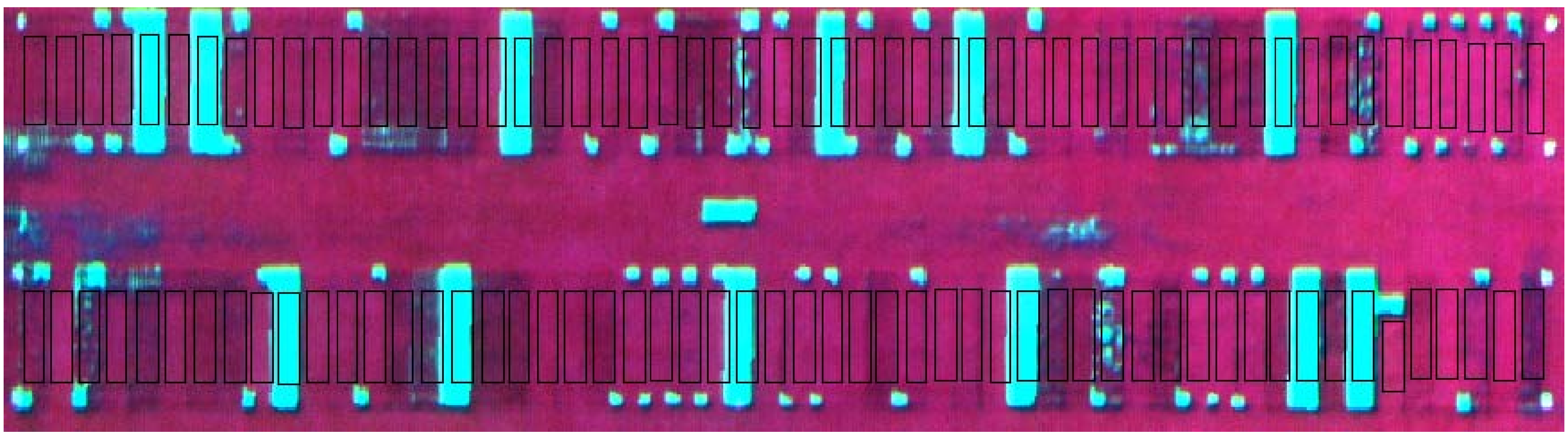

Figure 16. TPAC 2004 - Color infrared image taken August 16, 2004 at the R4 growth stage

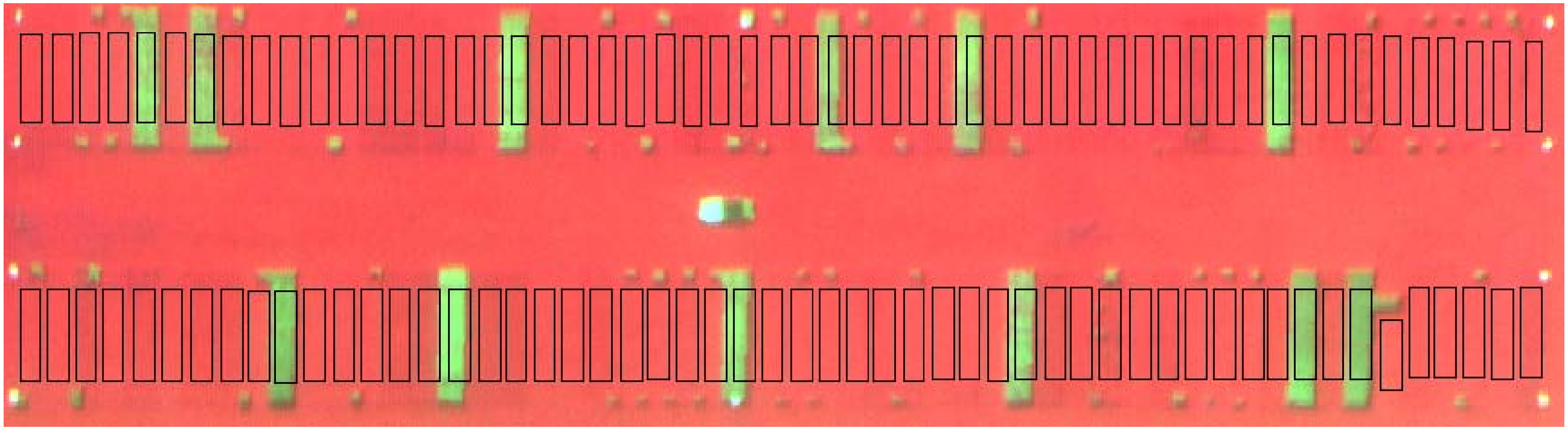

Figure 17. TPAC 2004 - Color infrared image taken August 30, 2004 at the R5 growth stage

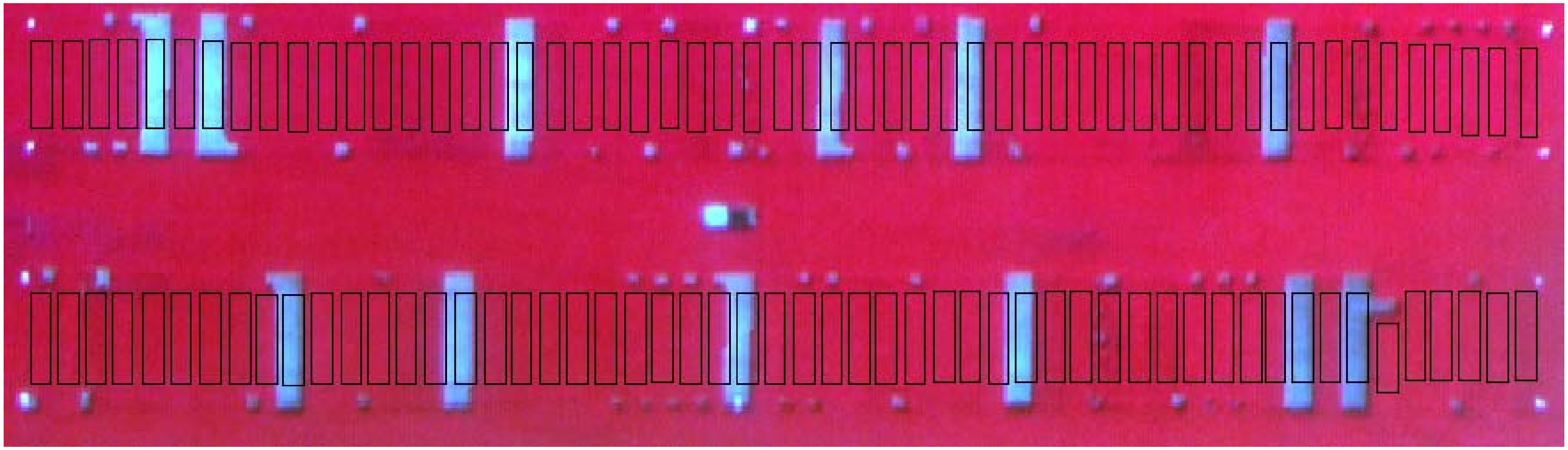

Figure 18. TPAC 2004 - Color infrared image taken September 7, 2004 at the R6 growth stage

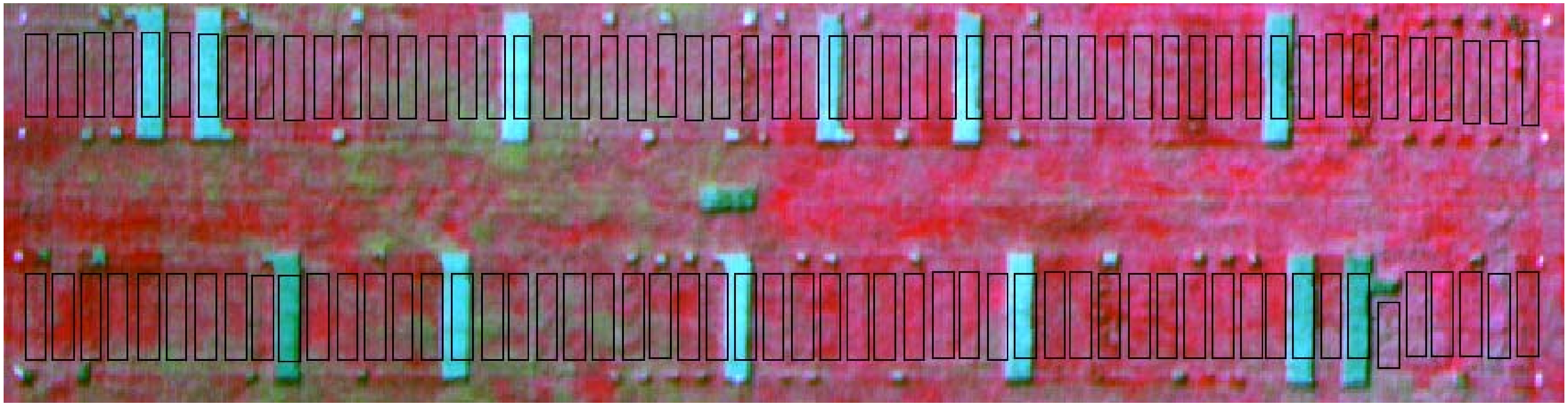

Figure 18. TPAC 2004 - Color infrared image taken September 22, 2004 at the R7 growth stage

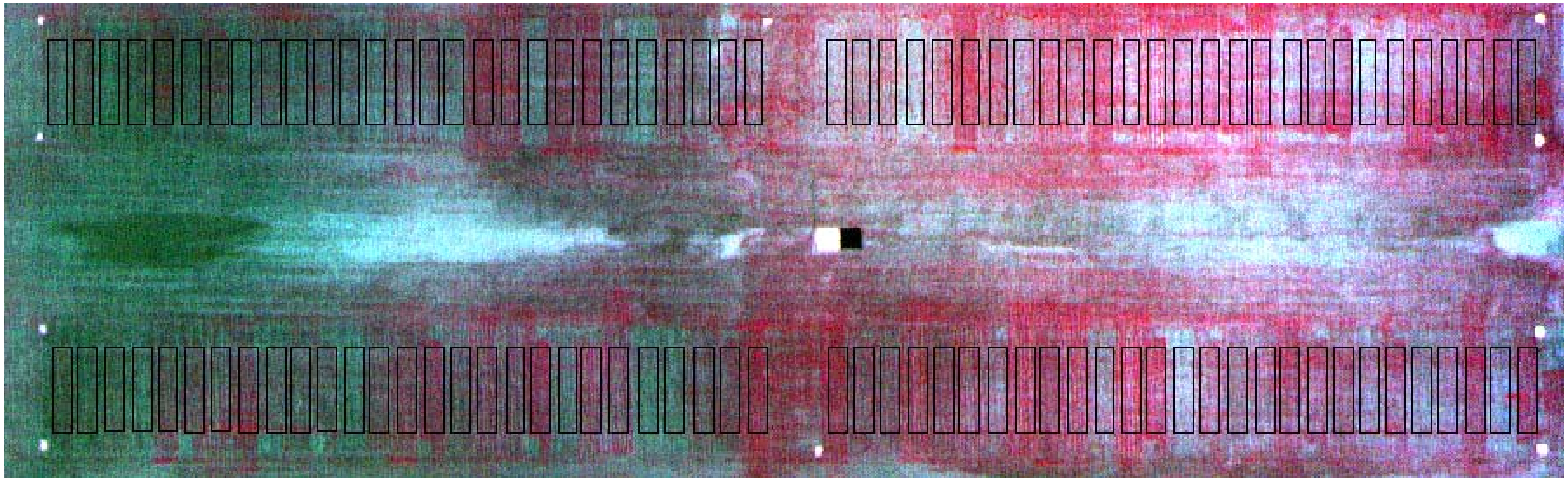

Figure 20. ACRE 2004 - Color infrared image taken July 1, 2004 at the V2 growth stage

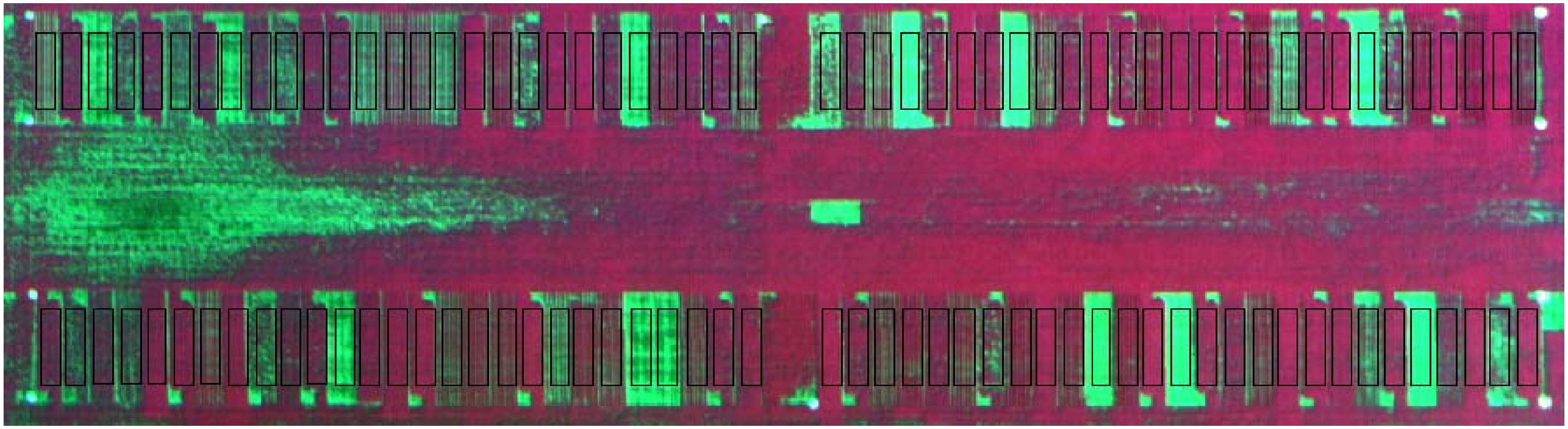

Figure 21. ACRE 2004 - Color infrared image taken July 22, 2004 at the R1 growth stage

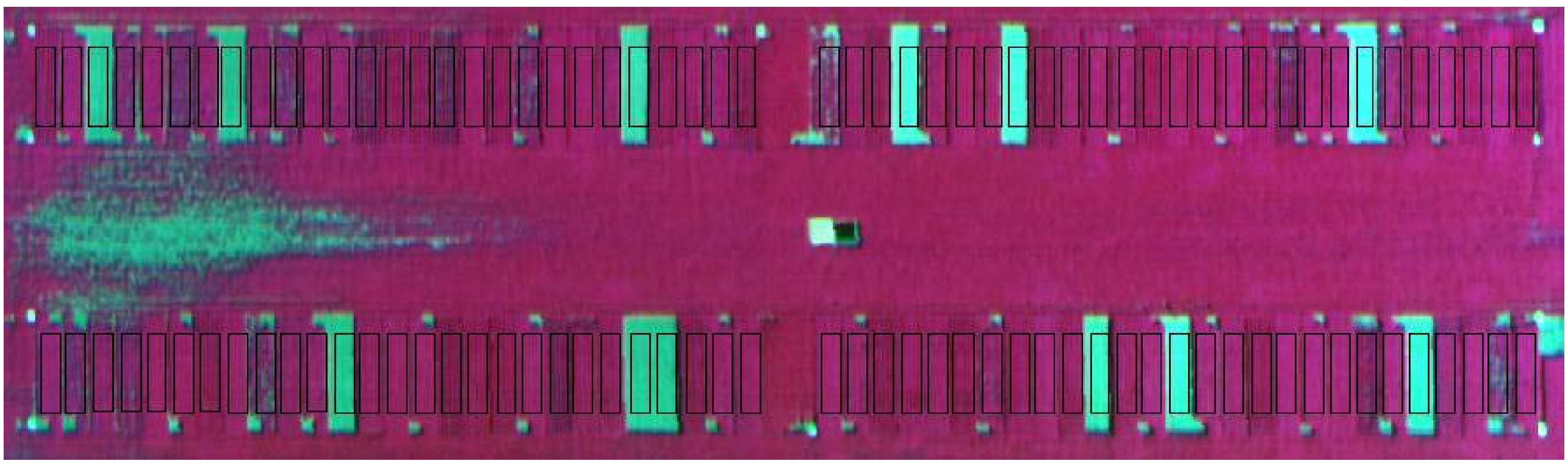

Figure 22. ACRE 2004 - Color infrared image taken August 3, 2004 at the R3 growth stage

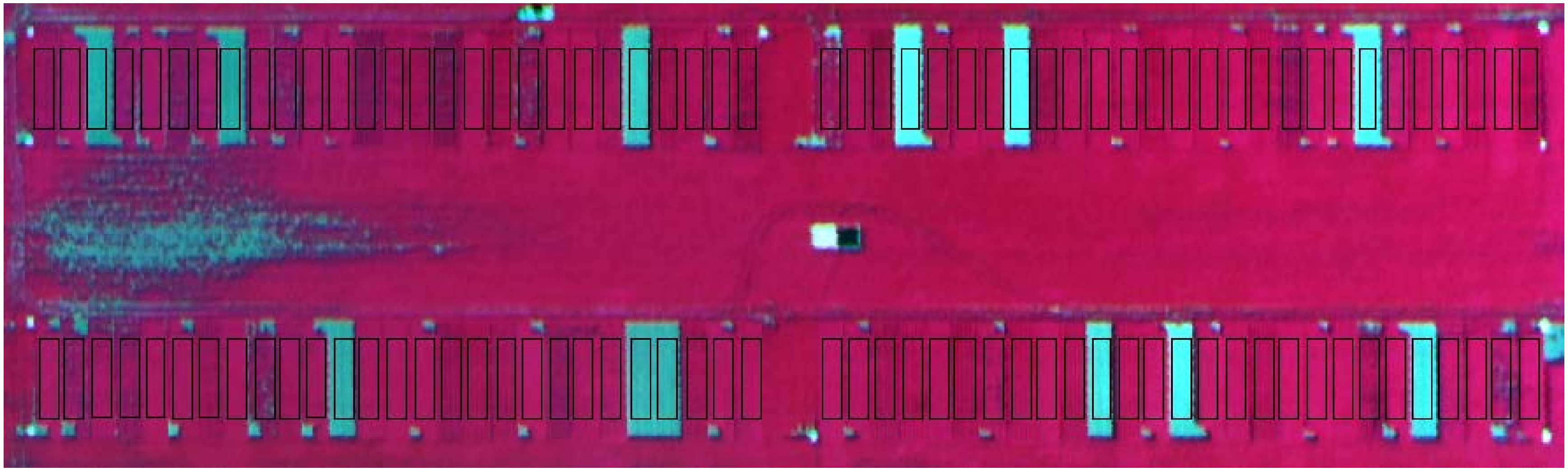

Figure 23. ACRE 2004 - Color infrared image taken August 16, 2004 at the R4 growth stage

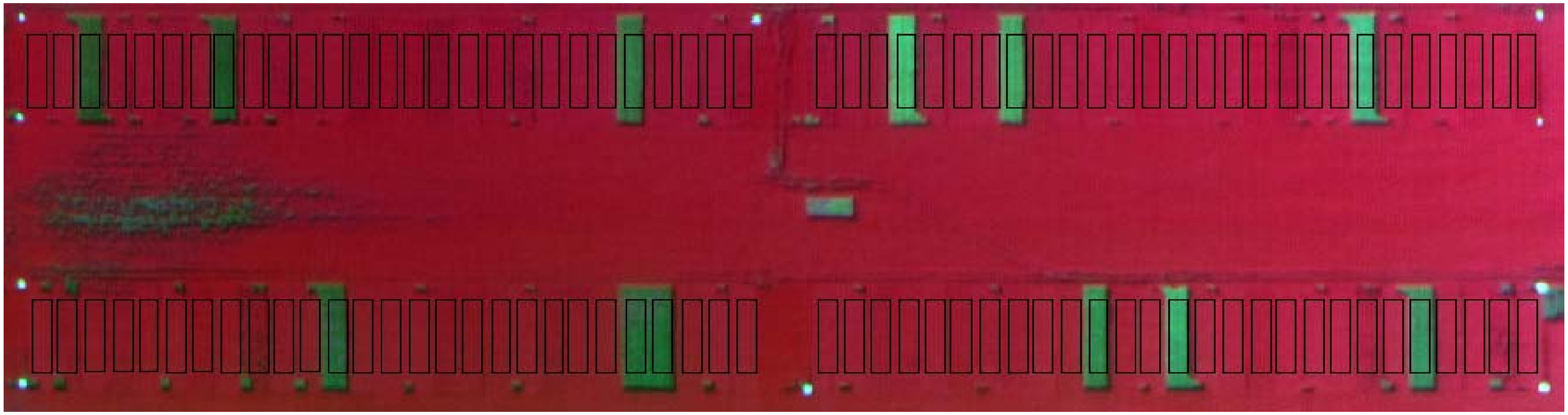

Figure 24. ACRE 2004 - Color infrared image taken August 30, 2004 at the R5 growth stage

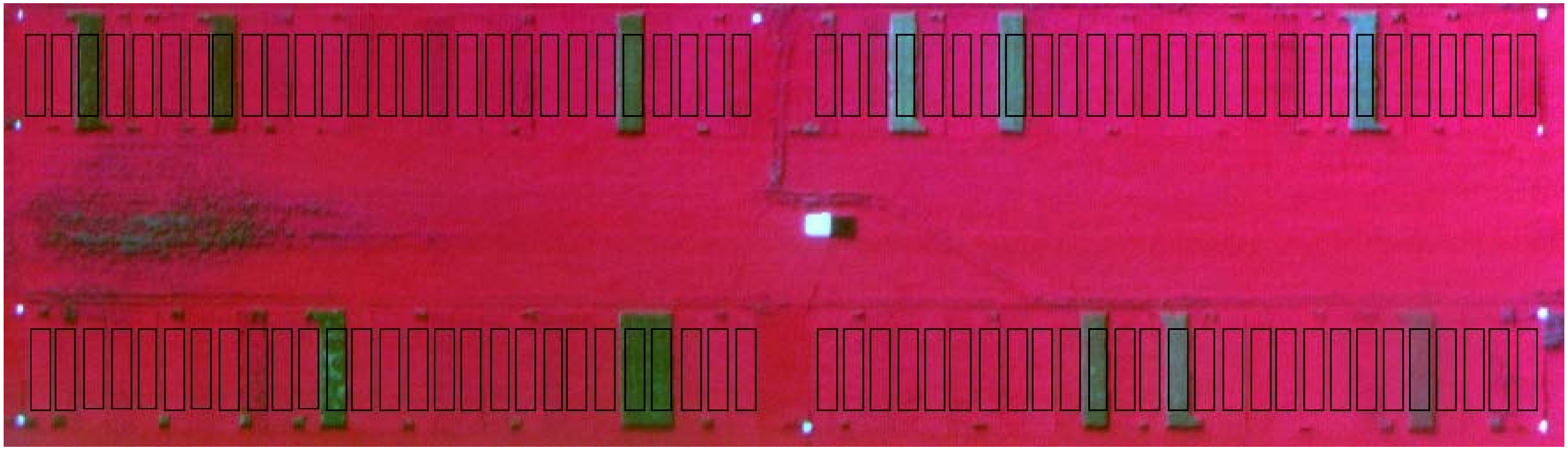

Figure 25. ACRE 2004 - Color infrared image taken September 7, 2004 at the R6 growth stage

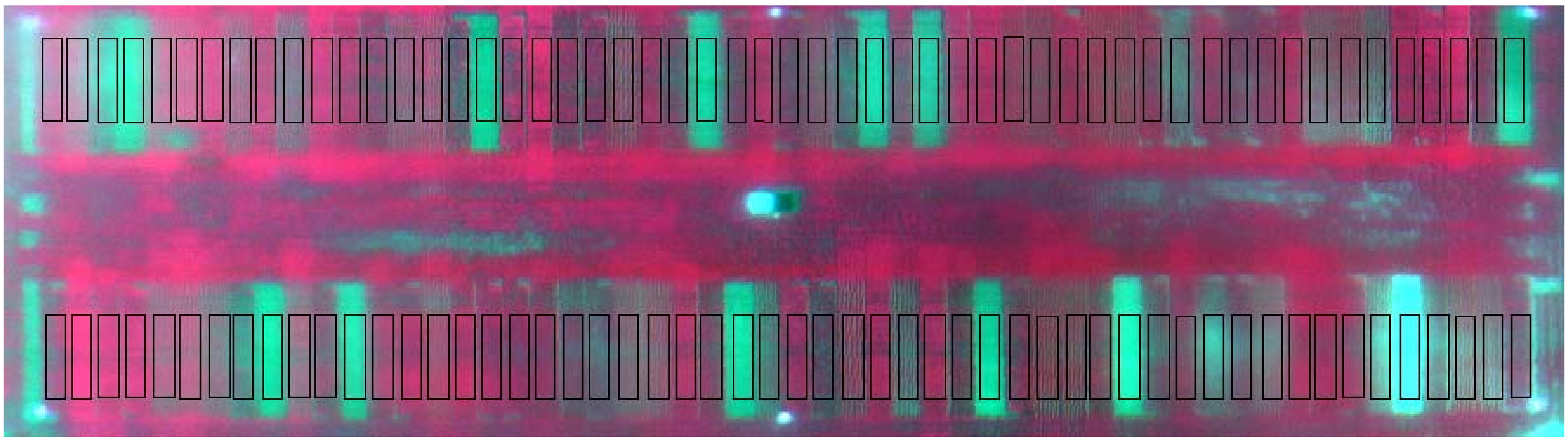

Figure 26. ACRE 2005 - Color infrared image taken June 29, 2005 at the V6 growth stage

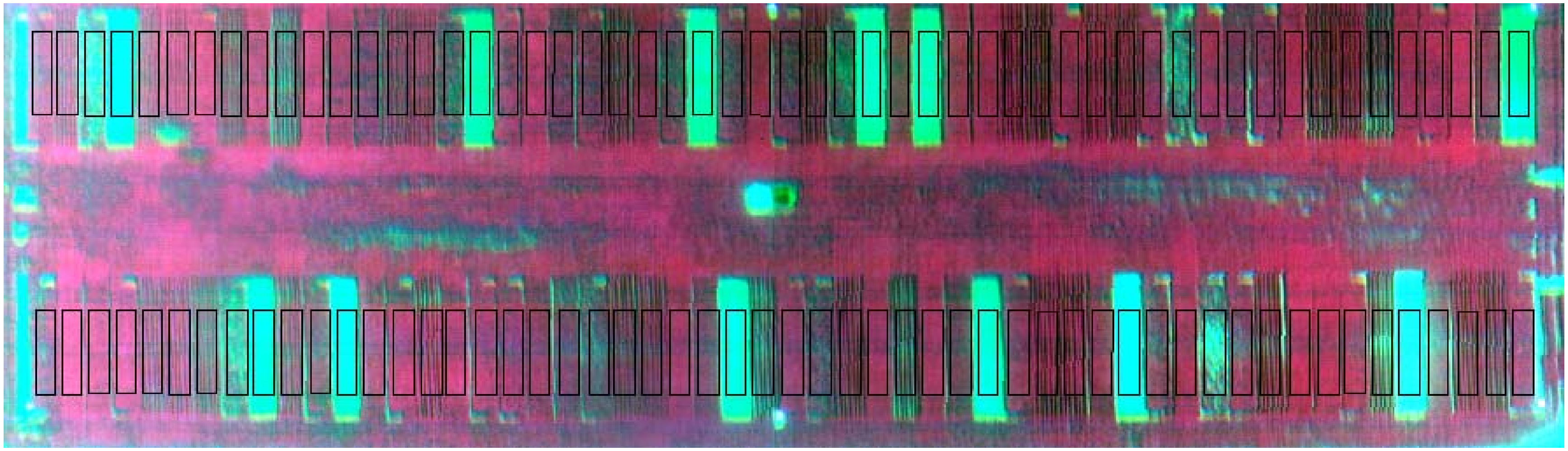

Figure 27. ACRE 2005 - Color infrared image taken July 7, 2005 at the R1 growth stage

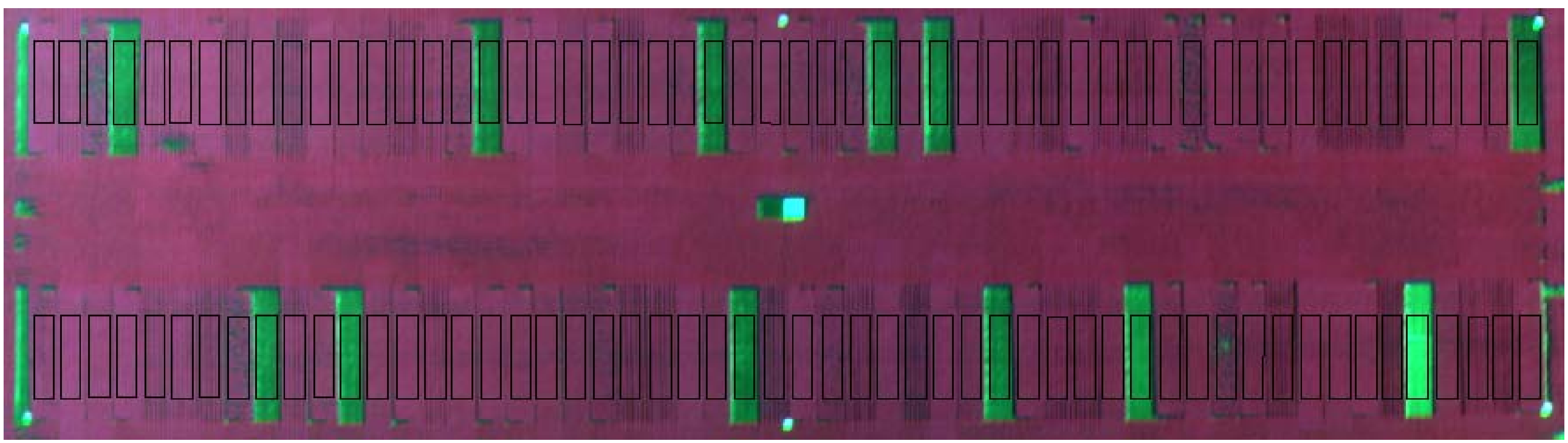

Figure 28. ACRE 2005 - Color infrared image taken July 19, 2005 at the R2 growth stage

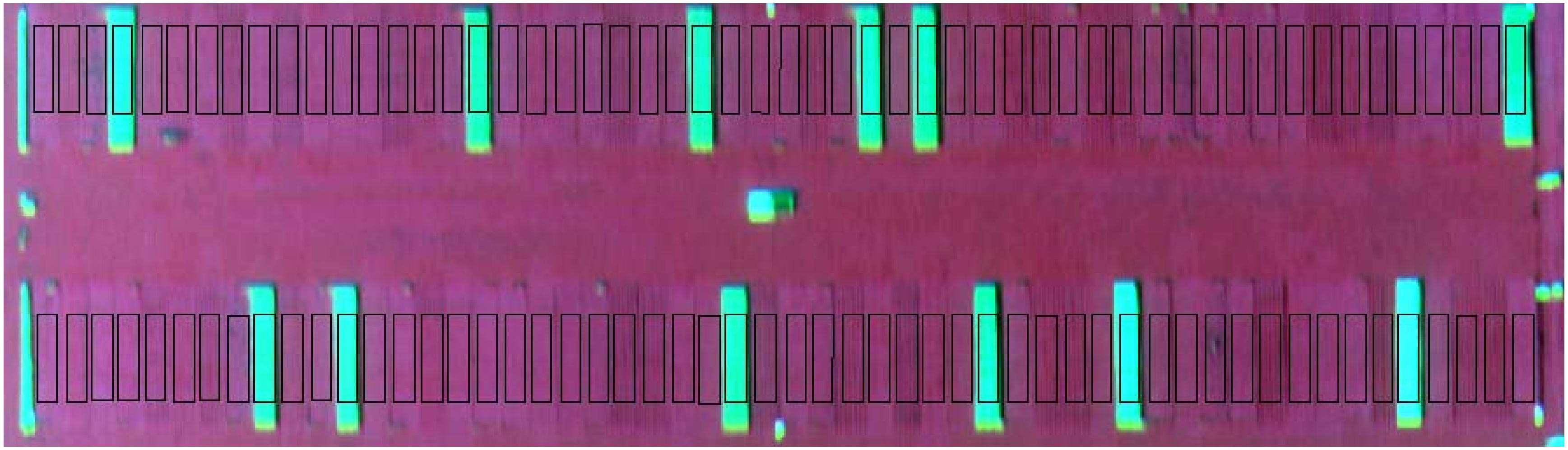

Figure 29. ACRE 2005 - Color infrared image taken July 29, 2005 at the R3 growth stage

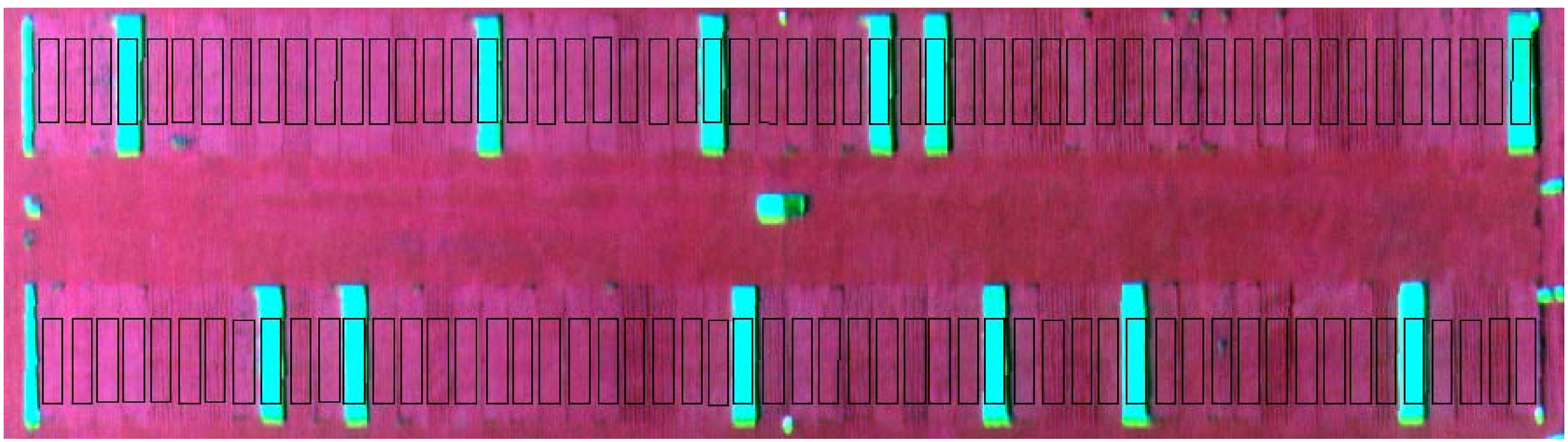

Figure 30. ACRE 2005 - Color infrared image taken August 3, 2005 at the R4 growth stage

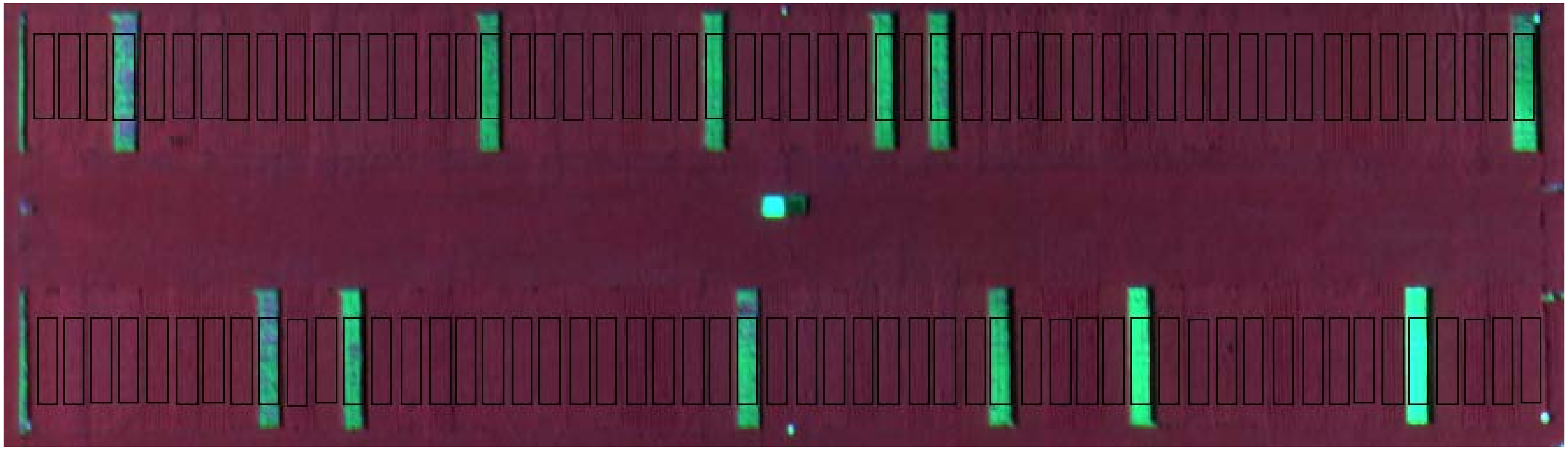

Figure 31. ACRE 2005 - Color infrared image taken August 21, 2005 at the R5 growth stage

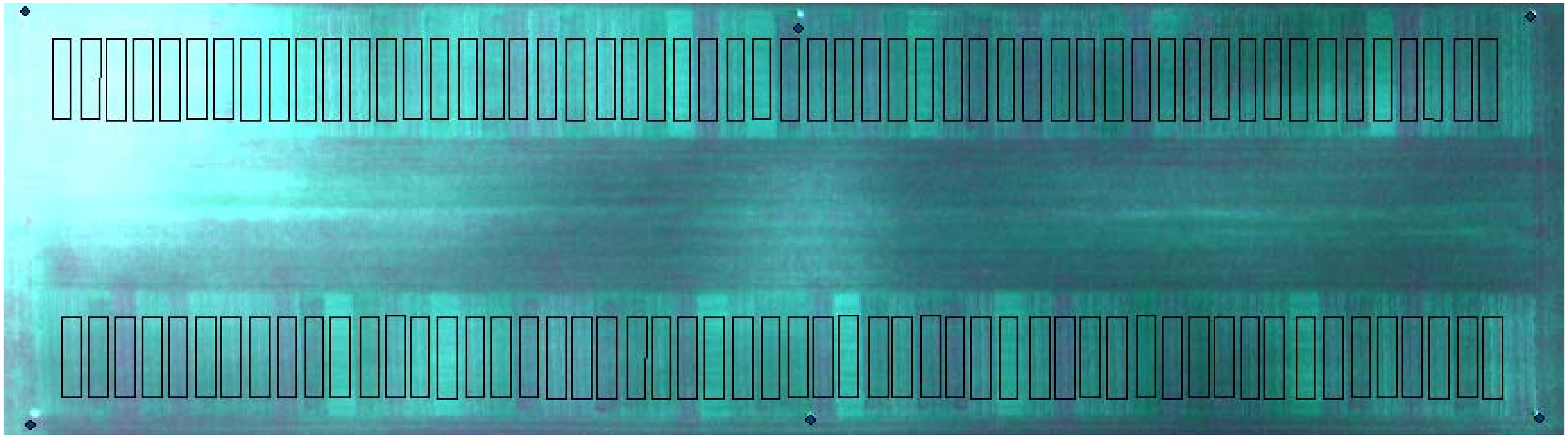

Figure 32. ACRE 2006 - Color infrared image taken June 29, 2006 at the V2 growth stage

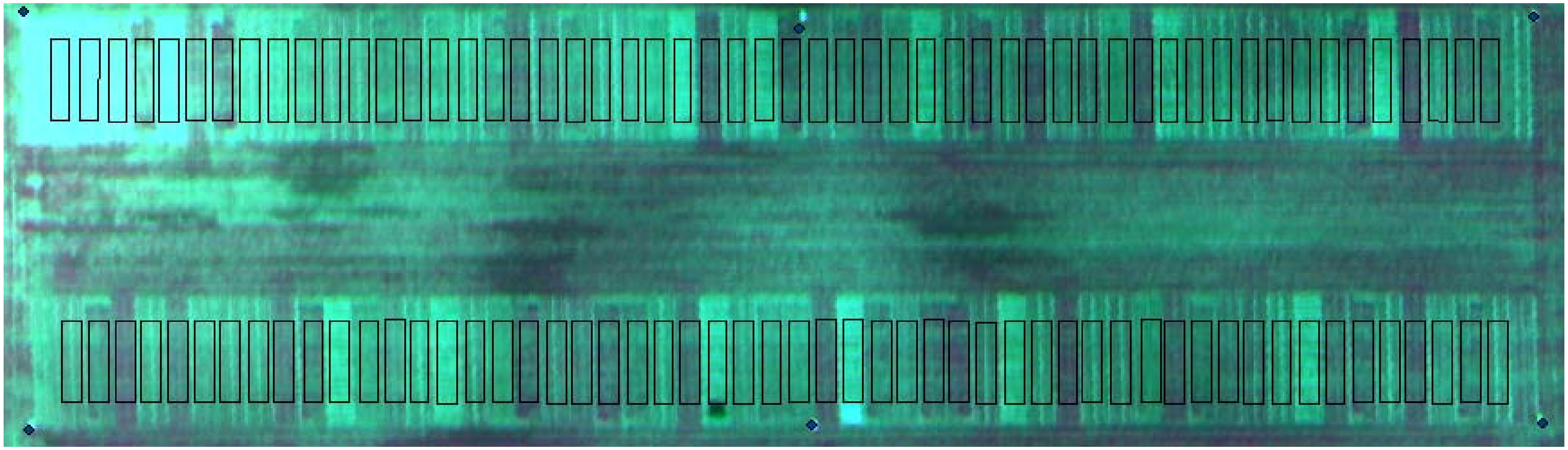

Figure 33. ACRE 2006 - Color infrared image taken July 7, 2006 at the V3 growth stage

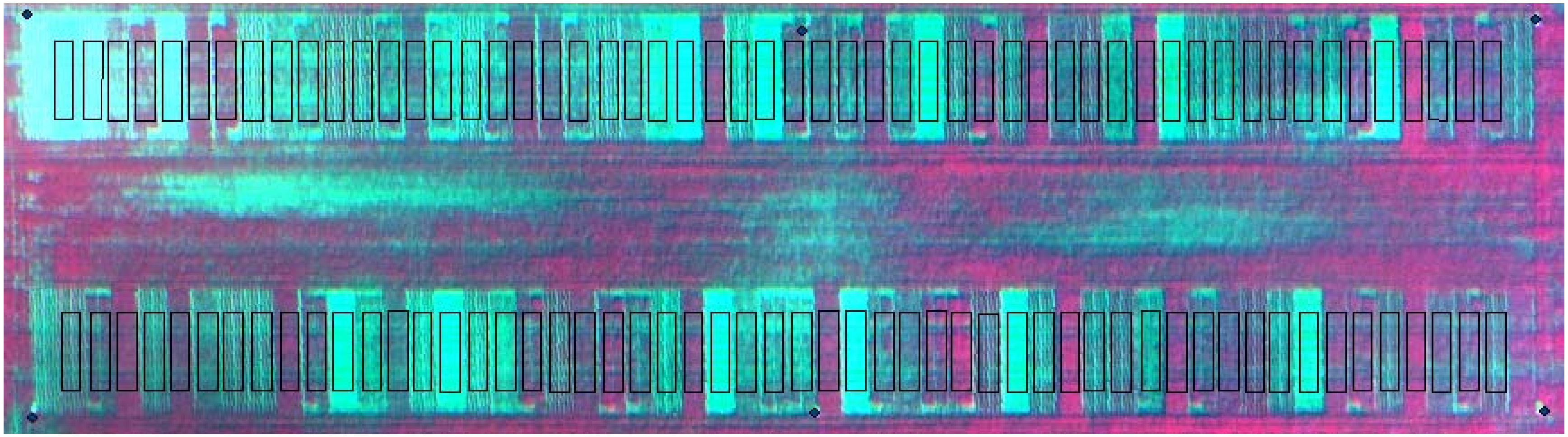

Figure 34. ACRE 2006 - Color infrared image taken June 15, 2006 at the V7 growth stage

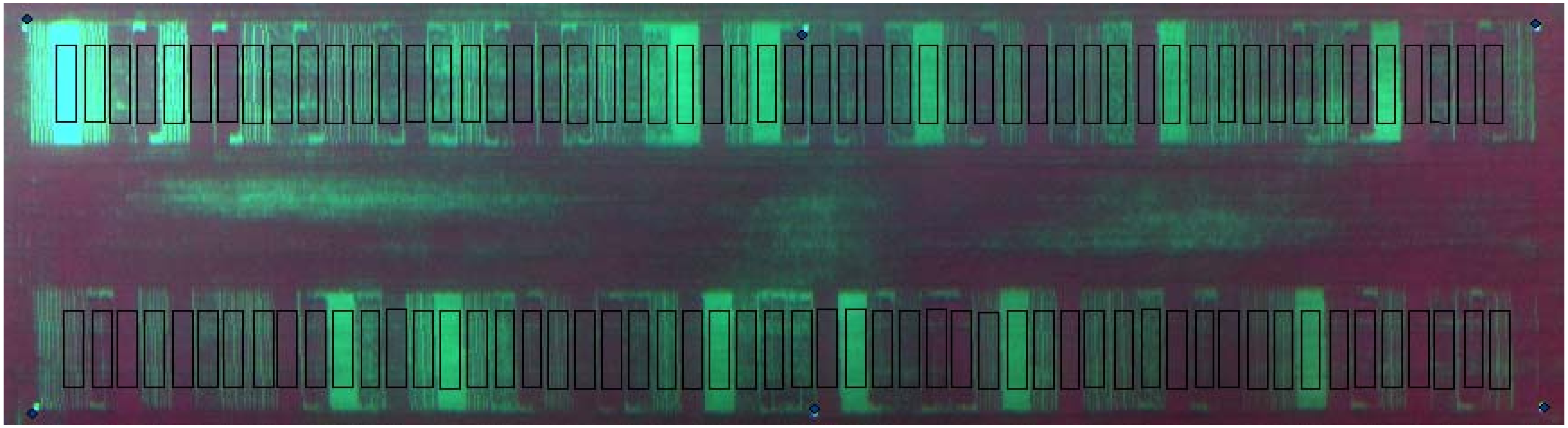

Figure 35. ACRE 2006 - Color infrared image taken July 24, 2006 at the R1 growth stage

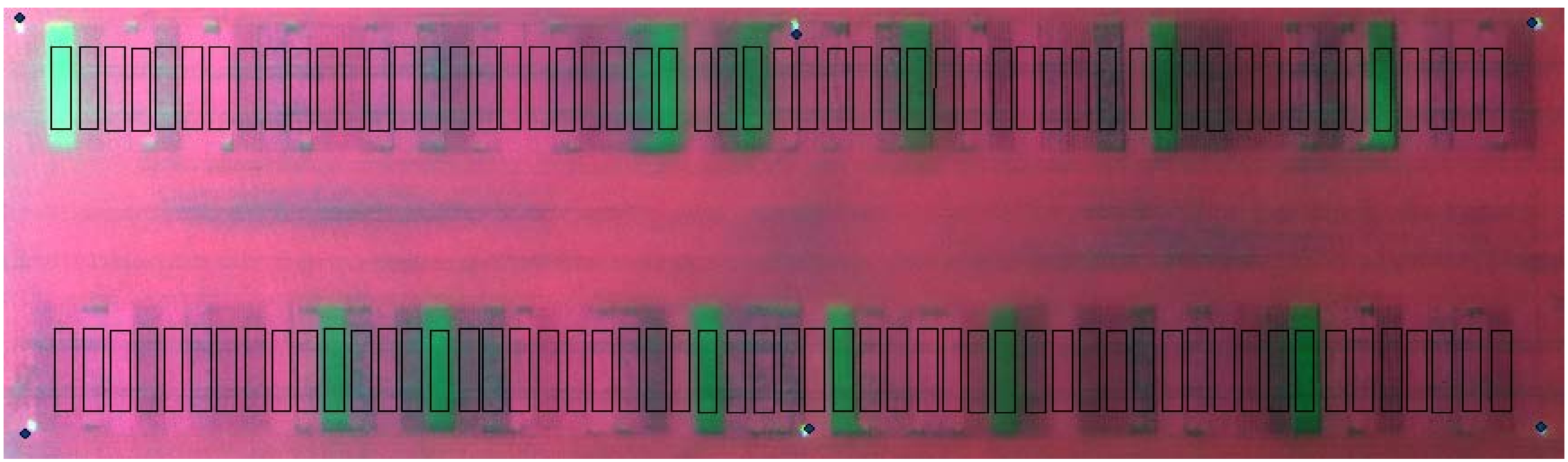

Figure 36. ACRE 2006 - Color infrared image taken July 30, 2006 at the R2 growth stage

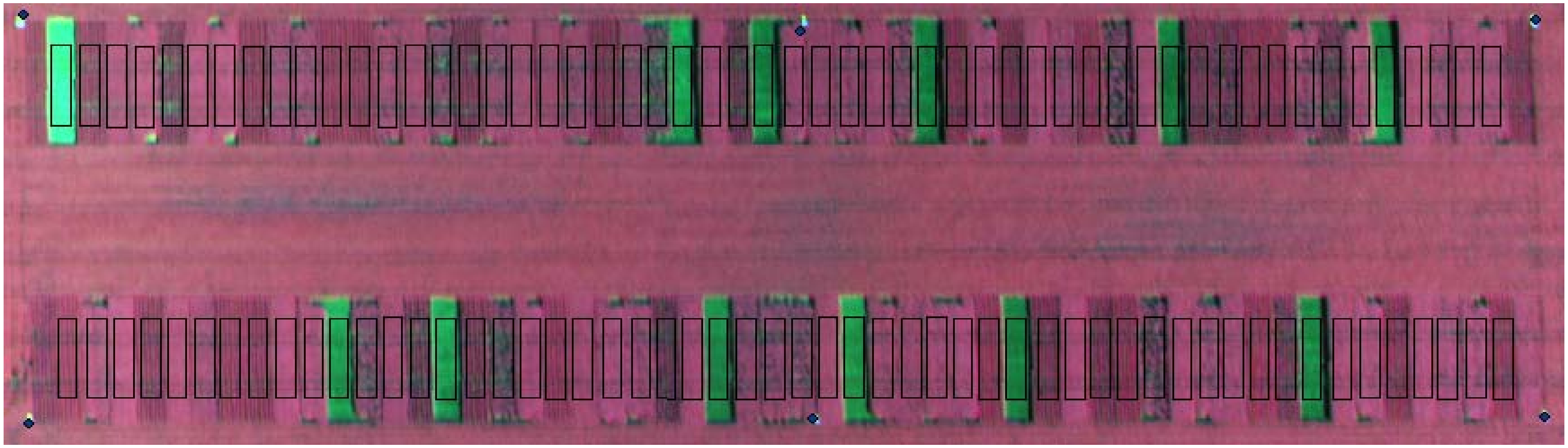

Figure 37. ACRE 2006 - Color infrared image taken August 4, 2006 at the R3 growth stage

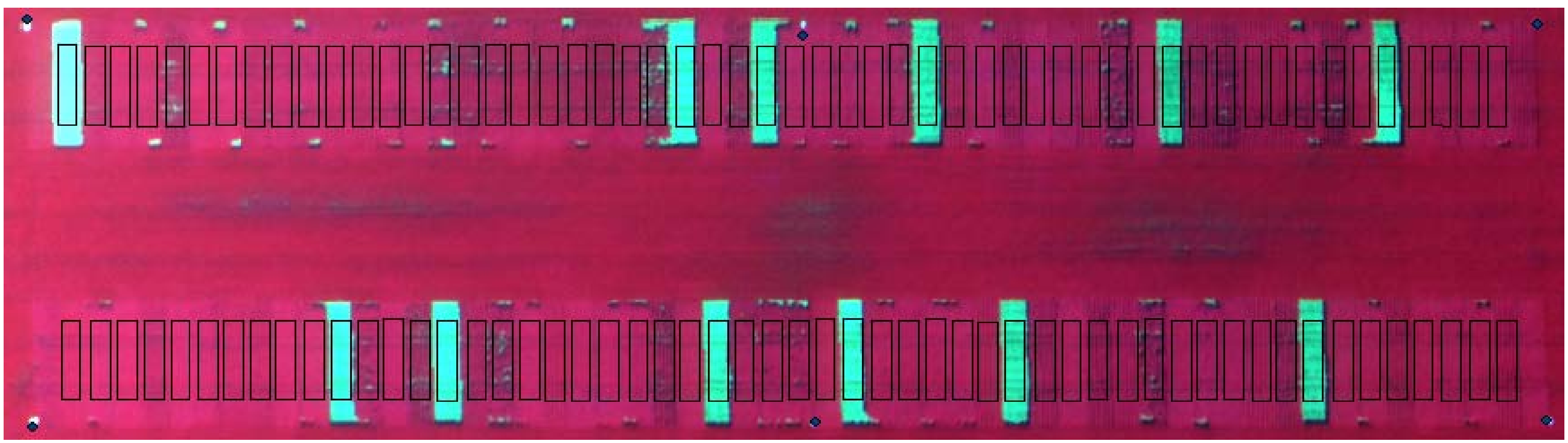

Figure 38. ACRE 2006 - Color infrared image taken August 22, 2006 at the R4 growth stage

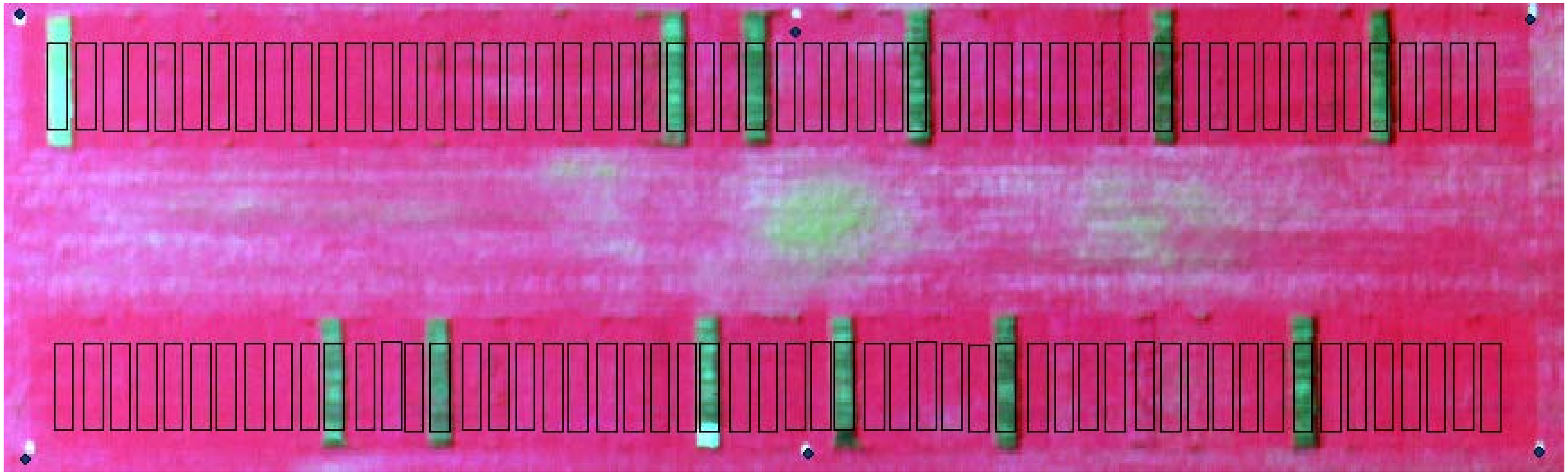

Figure 39. ACRE 2006 - Color infrared image taken September 15, 2006 at the R6 growth stage

Table 22. TPAC 2004 – best indices for 16cm treatments at R1								
Name	Growth Stage	Model	ProbF	RSq	ModSig	EstIntercept	EstX	EstXX
RVI	R1	XX	0.0000000000	0.9333	**	36.5367		116.8764
NIR	R1	XX	0.0000000000	0.9200	**	-450.0474		0.0559
GRVI	R1	XX	0.0000000000	0.9102	**	-129.1935		164.8411
Norm IR	R1	X_XX	0.0000000000	0.9207	**	298.8646	-1324.0025	4037.1019
GDVI	R1	X_XX	0.0000000000	0.9175	**	253.4326	4.9977	0.0641
NDVI	R1	X_XX	0.0000000000	0.9174	**	364.7160	545.8304	547.9507
OSAVI	R1	X_XX	0.0000000000	0.9174	**	364.7182	546.3981	549.0484
SAVI	R1	X_XX	0.0000000000	0.9173	**	364.7852	365.0575	244.9818
Norm R	R1	X_XX	0.0000000000	0.9101	**	3079.8589	-4717.5609	4490.0401
GOSAVI	R1	X_XX	0.0000000000	0.9039	**	251.4353	771.5089	1553.2202
GSAVI	R1	X_XX	0.0000000000	0.9038	**	251.4750	515.4317	693.1353
GVI	R1	X_XX	0.0000000000	0.9038	**	251.4660	770.6622	1549.7596
DVI	R1	X_XX	0.0000000000	0.8888	**	408.7921	3.1562	0.0142
SR	R1	X_XX	0.0000000001	0.8248	**	1113.9515	-314.7246	52.1184
Red	R1	X_XX	0.0000000001	0.8134	**	1609.1444	-7.7964	0.0227
Green	R1	X	0.0000001357	0.6353	**	1621.5856	-6.4775	
Norm G	R3	X	0.0000481424	0.3891	**	-4225.7988	5421.7247	

Table 23. TPAC 2004 – best indices for 36cm treatments at R1								
Name	Growth Stage	Model	ProbF	RSq	ModSig	EstIntercept	EstX	EstXX
NIR	R1	X_XX	0.0000000000	0.8710	**	1930.0960	-26.8366	0.2331
RVI	R1	XX	0.0000000000	0.8047	**	-64.1880		120.7046
Norm R	R1	X_XX	0.0000000006	0.7814	**	4417.3833	-7794.2754	8205.6563
NDVI	R1	X_XX	0.0000000008	0.7766	**	190.9530	672.1039	948.4026
SAVI	R1	X_XX	0.0000000008	0.7766	**	191.0041	449.6492	423.8582
OSAVI	R1	X_XX	0.0000000008	0.7765	**	191.0183	672.7446	949.8359
DVI	R1	X_XX	0.0000000011	0.7708	**	218.1650	4.6636	0.0250
RVI	R1	X	0.0000000014	0.7235	**	-247.7575	229.8238	
Norm IR	R1	X_XX	0.0000000019	0.7615	**	739.6416	-2964.5777	6764.6919
GDVI	R1	X_XX	0.0000000038	0.7498	**	119.5515	5.5243	0.0872
GRVI	R1	XX	0.0000000094	0.6847	**	-169.1334		158.2692
SR	V2	XX	0.0000000156	0.6146	**	1379.3960		-129.4420
GSAVI	R1	X_XX	0.0000000626	0.6942	**	130.5798	535.6552	936.0244
GOSAVI	R1	X_XX	0.0000000629	0.6941	**	130.5672	801.6989	2097.1663
Red	R1	X_XX	0.0000034372	0.5929	**	2020.6370	-11.8991	0.0366
Green	R4	X_XX	0.0001229564	0.4206	**	-5325.3919	52.7690	-0.2672
Norm G	R5	XX	0.0001401009	0.3512	**	3897.1498		-21862.460

Table 24. TPAC 2004 – best indices for 76cm treatments at R1								
Name	Growth Stage	Model	ProbF	RSq	ModSig	EstIntercept	EstX	EstXX
RVI	R1	XX	0.0000000000	0.8084	**	-14.1094		179.6512
Norm IR	R1	XX	0.0000000000	0.7639	**	-151.1722		1868.4515
NDVI	R1	X_XX	0.0000000000	0.7974	**	434.1061	611.6446	547.5211
OSAVI	R1	X_XX	0.0000000000	0.7973	**	434.0831	612.0838	548.3172
SAVI	R1	X_XX	0.0000000000	0.7973	**	434.0898	408.8116	244.5913
Norm R	R1	X_XX	0.0000000000	0.7910	**	3064.0669	-4426.4166	3961.7091
GRVI	R1	XX	0.0000000001	0.7382	**	-160.2198		166.0161
DVI	R1	X_XX	0.0000000002	0.7612	**	427.3028	2.9662	0.0117
NIR	R3	X_XX	0.0000000003	0.7337	**	7055.6403	-64.7008	0.3647
GVI	R1	X_XX	0.0000000004	0.7522	**	232.9621	799.0479	1654.8340
GSAVI	R1	X_XX	0.0000000004	0.7521	**	232.9826	534.5639	740.4352
GOSAVI	R1	X_XX	0.0000000004	0.7520	**	232.9583	799.7597	1657.8836
SR	R1	X_XX	0.0000000007	0.7433	**	1014.7203	-288.0584	47.5979
Red	R1	X_XX	0.0000000024	0.7223	**	1208.6898	-5.2336	0.0136
GDVI	R4	X_XX	0.0000000205	0.6580	**	-475.5570	5.6394	0.1448
Green	R1	X_XX	0.0000002888	0.6215	**	2668.5090	-20.5471	0.0972
Norm G	R4	X	0.0000009664	0.5111	**	10373.3571	-13652.245	

Table 25. ACRE 2004 – best indices for 19cm treatments at R1								
Name	Growth Stage	Model	ProbF	RSq	ModSig	EstIntercept	EstX	EstXX
RVI	R1	X	0.0000000000	0.7299	**	-737.2664	611.0984	
NDVI	R1	X	0.0000000001	0.7233	**	749.2708	920.1861	
OSAVI	R1	X	0.0000000001	0.7232	**	749.2309	920.8579	
SAVI	R1	X	0.0000000001	0.7231	**	749.1109	614.7770	
Norm R	R1	X	0.0000000001	0.7159	**	1633.2811	-1178.8132	
Norm G	R1	X	0.0000000002	0.7013	**	-451.0802	1256.6549	
DVI	R1	X_XX	0.0000000002	0.7393	**	764.4470	7.9233	0.0483
SR	R1	X_XX	0.0000000002	0.7382	**	2723.3107	-1029.2209	239.5848
Red	R1	X_XX	0.0000000008	0.7190	**	2307.8044	-12.1264	0.0381
GSAVI	R1	X	0.0000000012	0.6672	**	528.9234	-462.3304	
GOSAVI	R1	X	0.0000000012	0.6672	**	528.9868	-691.5647	
GVI	R1	X	0.0000000012	0.6671	**	529.0160	-690.6411	
GDVI	R1	X	0.0000000015	0.6632	**	504.0375	-5.3418	
GRVI	R1	X	0.0000000036	0.6458	**	1232.7131	-272.6870	
Green	R3	XX	0.0000000082	0.6287	**	-282.1406		0.0367
NIR	R4	XX	0.0000008801	0.5137	**	-238.6138		0.0272
Norm IR	R4	X	0.0000090522	0.4444	**	-418.5778	969.1397	

Table 26. ACRE 2004 – best indices for 38cm treatments at R1

Name	Growth Stage	Model	ProbF	RSq	ModSig	EstIntercept	EstX	EstXX
Norm G	R1	XX	0.0000000004	0.6893	**	-110.3617		2151.8948
GDVI	R1	X	0.0000000021	0.6572	**	448.5667	-4.9893	
RVI	R1	XX	0.0000000032	0.6485	**	-209.2840		364.6123
GSAVI	R1	X	0.0000000039	0.6442	**	472.7685	-432.3762	
GOSAVI	R1	X	0.0000000039	0.6441	**	472.8287	-646.7613	
GVI	R1	X	0.0000000039	0.6440	**	472.8775	-645.9392	
Norm R	R1	X_XX	0.0000000058	0.6833	**	3157.2874	-4433.8780	3862.8284
NDVI	R1	X	0.0000000167	0.6130	**	664.2546	836.3012	
OSAVI	R1	X	0.0000000168	0.6129	**	664.1915	836.8533	
SAVI	R1	X	0.0000000169	0.6128	**	664.1173	558.7033	
GRVI	R1	X_XX	0.0000000185	0.6601	**	2080.1734	-917.7035	249.9396
Green	R1	X	0.0000000361	0.5954	**	-427.5281	5.3534	
DVI	R1	X_XX	0.0000000423	0.6426	**	682.7416	8.8071	0.0629
SR	R1	X_XX	0.0000000442	0.6417	**	3034.4320	-1280.4591	331.8566
Red	R1	X_XX	0.0000001396	0.6158	**	2468.2238	-14.3923	0.0488
NIR	R4	XX	0.0000023392	0.4857	**	-241.1733		0.0269
Norm IR	R4	XX	0.0000043173	0.4673	**	-117.6724		1556.3671

Table 27. ACRE 2004 – best indices for 76cm treatments at R1

Name	Growth Stage	Model	ProbF	RSq	ModSig	EstIntercept	EstX	EstXX
Norm G	R1	XX	0.0000000001	0.7138	**	-124.1742		2489.0116
Norm R	R1	X	0.0000000002	0.6978	**	1627.9396	-1182.9335	
GDVI	R1	X	0.0000000006	0.6816	**	457.1743	-5.6965	
NDVI	R1	X	0.0000000006	0.6811	**	783.7604	941.4047	
OSAVI	R1	X	0.0000000006	0.6811	**	783.7045	942.1243	
SAVI	R1	X	0.0000000006	0.6810	**	783.3754	628.8272	
GSAVI	R1	X	0.0000000007	0.6770	**	464.7059	-460.6998	
GVI	R1	X	0.0000000007	0.6770	**	464.7392	-688.0750	
GOSAVI	R1	X	0.0000000007	0.6769	**	464.7350	-689.0419	
RVI	R1	X	0.0000000008	0.6750	**	-775.1027	654.4281	
DVI	R1	X_XX	0.0000000013	0.7109	**	807.3469	7.8761	0.0454
Red	R1	X_XX	0.0000000013	0.7100	**	2039.9170	-10.2495	0.0310
SR	R1	X	0.0000000024	0.6543	**	1405.9318	-284.7391	
GRVI	R1	X_XX	0.0000000031	0.6949	**	2164.1783	-954.7755	260.3822
Green	R1	X	0.0000000186	0.6106	**	-704.8620	7.3162	
NIR	R4	XX	0.0000006742	0.5211	**	-286.5607		0.0281
Norm IR	R4	XX	0.0000105513	0.4395	**	-122.2712		1338.9524

Table 28. ACRE 2005 – best indices for 19cm treatments at R1								
Name	Growth Stage	Model	ProbF	RSq	ModSig	EstIntercept	EstX	EstXX
GRVI	R1	X_XX	0.0000000000	0.8780	**	615.3434	-1070.9639	1138.3918
GOSAVI	R1	X_XX	0.0000000000	0.8765	**	755.7321	1970.4448	3009.1666
GVI	R1	X_XX	0.0000000000	0.8765	**	755.7237	1968.8936	3004.3810
GSAVI	R1	X_XX	0.0000000000	0.8764	**	755.6547	1315.8522	1342.0735
RVI	R1	XX	0.0000000000	0.8424	**	-71.5392		230.2983
SR	R1	XX	0.0000000000	0.8424	**	-71.5392		230.2983
Norm IR	R1	X_XX	0.0000000000	0.8606	**	686.5093	-3291.1260	9542.5066
GDVI	R1	X_XX	0.0000000000	0.8508	**	750.7700	10.3371	0.0832
NDVI	R1	X_XX	0.0000000000	0.8432	**	505.7454	915.2967	987.1370
SAVI	R1	X_XX	0.0000000000	0.8431	**	505.7688	611.7516	440.8628
OSAVI	R1	X_XX	0.0000000000	0.8431	**	505.7503	916.0797	988.7407
DVI	R1	X_XX	0.0000000000	0.8221	**	509.0611	4.4022	0.0205
Norm R	R1	X_XX	0.0000000000	0.8179	**	4998.2736	-8549.4244	8972.9851
NIR	R1	XX	0.0000000000	0.7593	**	-286.2386		0.0384
Red	R1	X	0.0000014270	0.5000	**	925.5219	-1.9951	
Norm G	R1	X_XX	0.0011366710	0.3369	**	-210741.55	482531.5702	-680405.9
Green	R1	XX	0.0028168175	0.2337	**	905.5975		-0.0183

Table 29. ACRE 2005 – best indices for 38cm treatments at R1								
Name	Growth Stage	Model	ProbF	RSq	ModSig	EstIntercept	EstX	EstXX
GSAVI	R1	X_XX	0.0000000002	0.7418	**	728.2360	1872.3046	2305.8752
GVI	R1	X_XX	0.0000000002	0.7418	**	728.2271	2800.1697	5157.7570
GOSAVI	R1	X_XX	0.0000000002	0.7417	**	728.1867	2802.4666	5166.7373
GRVI	R1	X_XX	0.0000000002	0.7406	**	1351.1538	-2048.3538	1797.4193
GDVI	R1	X_XX	0.0000000003	0.7329	**	726.7580	14.7803	0.1521
Norm IR	R1	X_XX	0.0000000009	0.7165	**	1588.2815	-6820.5727	16567.0811
RVI	R1	XX	0.0000000018	0.6598	**	-118.2630		230.2346
SR	R1	XX	0.0000000018	0.6598	**	-118.2630		230.2346
SAVI	R1	X_XX	0.0000000049	0.6862	**	410.9604	861.1657	794.9218
NDVI	R1	X_XX	0.0000000050	0.6861	**	410.9716	1287.9082	1778.8628
OSAVI	R1	X_XX	0.0000000050	0.6861	**	410.9766	1288.9951	1781.7074
DVI	R1	X_XX	0.0000000060	0.6825	**	421.3447	6.8348	0.0422
Norm R	R1	X_XX	0.0000000454	0.6411	**	7598.6110	-14130.7814	15850.4719
NIR	R1	XX	0.0000000682	0.5803	**	-262.8527		0.0372
Norm G	R2	XX	0.0000078260	0.4489	**	-1944.4532		9717.7801
Red	R1	X	0.0000280479	0.4075	**	1051.4680	-2.3661	
Green	R2	X_XX	0.0006173164	0.3610	**	-5341.6807	52.1250	-0.2785

Table 30. ACRE 2005 – best indices for 76cm treatments at R1

Name	Growth Stage	Model	ProbF	RSq	ModSig	EstIntercept	EstX	EstXX
GRVI	R1	X_XX	0.0000000010	0.7159	**	1656.5704	-2588.9903	2331.7321
GOSAVI	R1	X_XX	0.0000000017	0.7056	**	951.9135	3217.4091	5491.4967
GSAVI	R1	X_XX	0.0000000018	0.7053	**	951.4879	2146.7982	2446.4776
GVI	R1	X_XX	0.0000000018	0.7052	**	951.5620	3212.3828	5477.5452
Norm IR	R1	X_XX	0.0000000041	0.6899	**	1562.2891	-6979.8102	17833.5429
RVI	R1	XX	0.0000000043	0.6424	**	-132.4271		282.7833
SR	R1	XX	0.0000000043	0.6424	**	-132.4271		282.7833
OSAVI	R1	X_XX	0.0000000124	0.6682	**	573.3535	1408.0950	1766.7726
NDVI	R1	X_XX	0.0000000124	0.6682	**	573.3799	1407.0629	1764.2646
SAVI	R1	X_XX	0.0000000125	0.6681	**	573.3447	940.1741	787.5799
Norm R	R1	X_XX	0.0000000526	0.6379	**	7756.1423	-13960.9017	15276.4837
GDVI	R1	X_XX	0.0000002515	0.6019	**	794.6443	10.4604	0.0715
DVI	R1	X_XX	0.0000003047	0.5972	**	569.3530	5.3375	0.0242
NIR	R1	X	0.0000071388	0.4518	**	-839.7798	6.3643	
Red	R1	X	0.0001776234	0.3425	**	915.8749	-1.8216	
Norm G	R1	X_XX	0.0006518288	0.3589	**	-404011.87	929274.9457	-1317465.8
Green	R3	X	0.0090162866	0.1841	**	1090.5823	-2.9650	

Table 31. ACRE 2006 – best indices for 19cm treatments at R1

Name	Growth Stage	Model	ProbF	RSq	ModSig	EstIntercept	EstX	EstXX
GRVI	R1	X_XX	0.0000000010	0.7159	**	1656.5704	-2588.9903	2331.7321
GOSAVI	R1	X_XX	0.0000000017	0.7056	**	951.9135	3217.4091	5491.4967
GSAVI	R1	X_XX	0.0000000018	0.7053	**	951.4879	2146.7982	2446.4776
GVI	R1	X_XX	0.0000000018	0.7052	**	951.5620	3212.3828	5477.5452
Norm IR	R1	X_XX	0.0000000041	0.6899	**	1562.2891	-6979.8102	17833.5429
RVI	R1	XX	0.0000000043	0.6424	**	-132.4271		282.7833
SR	R1	XX	0.0000000043	0.6424	**	-132.4271		282.7833
OSAVI	R1	X_XX	0.0000000124	0.6682	**	573.3535	1408.0950	1766.7726
NDVI	R1	X_XX	0.0000000124	0.6682	**	573.3799	1407.0629	1764.2646
SAVI	R1	X_XX	0.0000000125	0.6681	**	573.3447	940.1741	787.5799
Norm R	R1	X_XX	0.0000000526	0.6379	**	7756.1423	-13960.9017	15276.4837
GDVI	R1	X_XX	0.0000002515	0.6019	**	794.6443	10.4604	0.0715
DVI	R1	X_XX	0.0000003047	0.5972	**	569.3530	5.3375	0.0242
NIR	R1	X	0.0000071388	0.4518	**	-839.7798	6.3643	
Red	R1	X	0.0001776234	0.3425	**	915.8749	-1.8216	
Norm G	R1	X_XX	0.0006518288	0.3589	**	-404011.87	929274.9457	-1317465.8
Green	R3	X	0.0090162866	0.1841	**	1090.5823	-2.9650	

Table 32. ACRE 2006 – best indices for 38cm treatments at R1								
Name	Growth Stage	Model	ProbF	RSq	ModSig	EstIntercept	EstX	EstXX
GRVI	V7	XX	0.0000000000	0.8130	**	-193.5695		365.9779
GSAVI	V7	X_XX	0.0000000000	0.8140	**	696.3471	857.3410	629.9689
GVI	V7	X_XX	0.0000000000	0.8140	**	696.1761	1280.7200	1405.6010
GOSAVI	V7	X_XX	0.0000000000	0.8139	**	696.1999	1282.2506	1409.0597
Norm IR	V7	XX	0.0000000000	0.7724	**	-157.9064		2876.1968
GDVI	V7	X_XX	0.0000000000	0.8042	**	688.0456	8.3416	0.0569
OSAVI	V7	X	0.0000000000	0.7465	**	565.5716	441.8601	
NDVI	V7	X	0.0000000000	0.7465	**	565.6083	441.5373	
SAVI	V7	X	0.0000000000	0.7464	**	565.4925	295.0325	
RVI	V7	X	0.0000000000	0.7450	**	-224.2956	334.4454	
SR	V7	X	0.0000000000	0.7450	**	-224.2956	334.4454	
Norm R	V7	X	0.0000000001	0.7132	**	1560.3115	-1246.3098	
DVI	V7	X_XX	0.0000000005	0.7274	**	572.6516	3.3531	0.0118
Red	V7	X_XX	0.0000000290	0.6507	**	1466.7813	-6.3275	0.0165
NIR	R3	XX	0.0000001817	0.5558	**	-80.2389		0.0227
Green	V7	X_XX	0.0000288334	0.4693	**	3109.7036	-19.2712	0.0708
Norm G	R1	X_XX	0.0004612862	0.3722	**	-133752.21	328436.1155	-496320.11

Table 33. ACRE 2006 – best indices for 76cm treatments at R1								
Name	Growth Stage	Model	ProbF	RSq	ModSig	EstIntercept	EstX	EstXX
RVI	R2	XX	0.0000000000	0.8145	**	-62.2987		41.9169
SR	R2	XX	0.0000000000	0.8145	**	-62.2987		41.9169
GDVI	R2	X	0.0000000000	0.8023	**	24.2069	2.6772	
GRVI	R3	X_XX	0.0000000000	0.8231	**	216.9573	-261.6483	192.3853
Norm IR	R2	X_XX	0.0000000000	0.8207	**	863.6742	-2473.4335	4368.2722
GSAVI	R3	X_XX	0.0000000000	0.8136	**	36.6233	215.1976	466.2005
GOSAVI	R3	X_XX	0.0000000000	0.8136	**	36.5703	322.1979	1043.4597
GVI	R3	X_XX	0.0000000000	0.8135	**	36.5545	321.9155	1040.9893
SAVI	R2	X_XX	0.0000000000	0.8130	**	31.1991	115.4921	256.7686
OSAVI	R2	X_XX	0.0000000000	0.8129	**	31.1473	172.8135	576.2280
NDVI	R2	X_XX	0.0000000000	0.8129	**	31.1378	172.6491	575.3518
DVI	R3	X_XX	0.0000000000	0.8090	**	61.6878	1.8219	0.0250
Norm R	R3	X_XX	0.0000000000	0.8018	**	2208.2534	-4242.9249	4883.6225
NIR	R3	X	0.0000000008	0.6759	**	-150.3179	1.8315	
Norm G	R4	XX	0.0000022270	0.4871	**	1252.6941		-3981.5704
Red	R4	X	0.0000105165	0.4396	**	281.5628	-0.5931	
Green	V7	X_XX	0.0001589871	0.4115	**	2330.4114	-16.5228	0.0738